

The long-term thermal consequences of rifting: implications for basin reactivation

M. Sandiford,* S. Frederiksen[†] and J. Braun[†]

*School of Earth Sciences, University of Melbourne,
Victoria, 3010, Australia

[†]Research School of Earth Sciences, Australian National
University, Canberra, ACT 0200, Australia

ABSTRACT

The attenuation of the continental crust during rifting and the subsequent filling of the rift-related accommodation alter the long-term thermal and mechanical state of the lithosphere. This is primarily because the Moho is shallowed due to density contrasts between the sediment fill and the crust, but also reflects the attenuation of the pre-existing crustal heat production and its burial beneath the basin, as well the thermal properties of the basin fill. Moho shallowing and attenuation of pre-existing heat production contribute to long-term cooling of the Moho and thus lithospheric strengthening, as has been pointed out in many previous studies. In contrast, basin filling normally contributes to significant Moho heating allowing the possibility of long-term lithospheric weakening, the magnitude of which is dependent on the thermal properties of the basin-fill and the distribution of heat sources in the crust. This paper focuses on the thermal property structure of the crust and basin-fill in effecting long-term changes in lithospheric thermal regime, with particular emphasis on the distribution of heat producing elements in the crust. The parameter space appropriate to typical continental crust is explored using a formalism for the heat production distributions that makes no priori assumptions about the specific form of the distribution. The plausible parameter space allows a wide range in potential long-term thermal responses. However, with the proviso that the accommodation created by the isostatic response to rifting is essentially filled, the long-term thermal response to rift basin formation will generally increase average crustal thermal gradients beneath basins but cool the Moho due to its reduction in depth. The increase in the average crustal thermal gradient induces lateral heat flow that necessarily heats the Moho along basin margins, especially in narrow rift basins. Using coupled thermo-mechanical models with temperature sensitive creep-parameters, we show that such heating may be sufficient to localise subsequent deformation in the vicinity of major basin bounding structures, potentially explaining the offset observed in some stacked rift basin successions.

INTRODUCTION

The notion of reactivation of continental crust is familiar to geologists who study continental interiors. In many instances, tectonic activity seems to be localised along discrete structures or within defined zones that are thus inferred to be weaker than the surrounding, more inert crustal domains (e.g. Cooper & Williams, 1989; Buchanan & Buchanan, 1995; Zeigler *et al.*, 1995). Crustal strength heterogeneities are to be expected given the compositional and structural heterogeneity of the continental crust, and selective reactivation within continental interiors is usually attributed to the existence of pre-existing structural anisotropy as may occur, for example, as a consequence of fabric development during earlier or ongoing deformation

(e.g. Sibson, 1995; Frederiksen & Braun, 2001). In addition to the influence of composition and fabric, the bulk strength of the lithosphere is also sensitive to thermal regime (e.g. Brace & Kohlstedt, 1980; Ord & Hobbs, 1989) with subtle variations in thermal structure potentially leading to variations in strength sufficient to localise deformation. Models of lithospheric rheology based on extrapolation of laboratory data show extraordinary temperature sensitivity (e.g. Brace & Kohlstedt, 1980; Ord & Hobbs, 1989), but remain to be validated by independent constraints derived from observations of the natural tectonic deformation of the lithosphere. These considerations suggest that interpretations of the factors controlling localisation of strain at the lithospheric scale may be difficult to isolate unambiguously, as highlighted by ongoing debate concerning the factors that govern the development of stacked rift basins as well as basin inversion (e.g. Lowell, 1995; Sandiford, 1999; Hansen & Nielsen, 2002).

Correspondence: Mike Sandiford, School of Earth Sciences, University of Melbourne, Victoria, 3010, Australia. E-mail: mikes@unimelb.edu.au

Deformation of the continental crust and the consequent surface processes that restore the crust to normal thickness lead to long-term changes in the compositional structure of the lithosphere. For example, since basin-filling sediments are typically significantly lighter than continental crust, attenuation of continental crust during rifting should lead to a long-term reduction in the Moho depth even in the cases where the accommodation associated with the subsidence is entirely filled with sediment. Changes in the composition of the lithosphere can lead to marked changes in the long-term strength of the lithosphere, and thus impact on its response during subsequent tectonic events. In the case of rifted continental crust, the long-term shallowing of the Moho has been equated with significant increases in lithospheric strength (England, 1983; Braun, 1992; Van Wees & Stephenson, 1995; Ziegler *et al.*, 1995; Bertotti *et al.*, 1997). While such

long-term increases in lithospheric strength may explain the observation that some basins show significant changes in the locus of deformation during successive rifting events separated in time by at least 50 Myr, there are also examples of stacked rift basins in which a similar temporal sequence of deformation seems to have been repeatedly localised in the one place (e.g. the Mt. Isa Rift Basin, Eriksson *et al.*, 1993; O'Dea *et al.*, 1997). In some settings, successive rift sequences show only limited offset (Fig. 1, Paul *et al.*, 1999) suggesting some inherent correlation length-scale involved in the long term structuring of the crust. Similarly, the common occurrence of basin-inversion seems to imply that basins are capable of remaining relatively weak long-after formation (see Sandiford, 1999 for further discussion). The time-interval between successive rifting events is important. In the short term (< 50 Myr) lithospheric thermal regimes will reflect

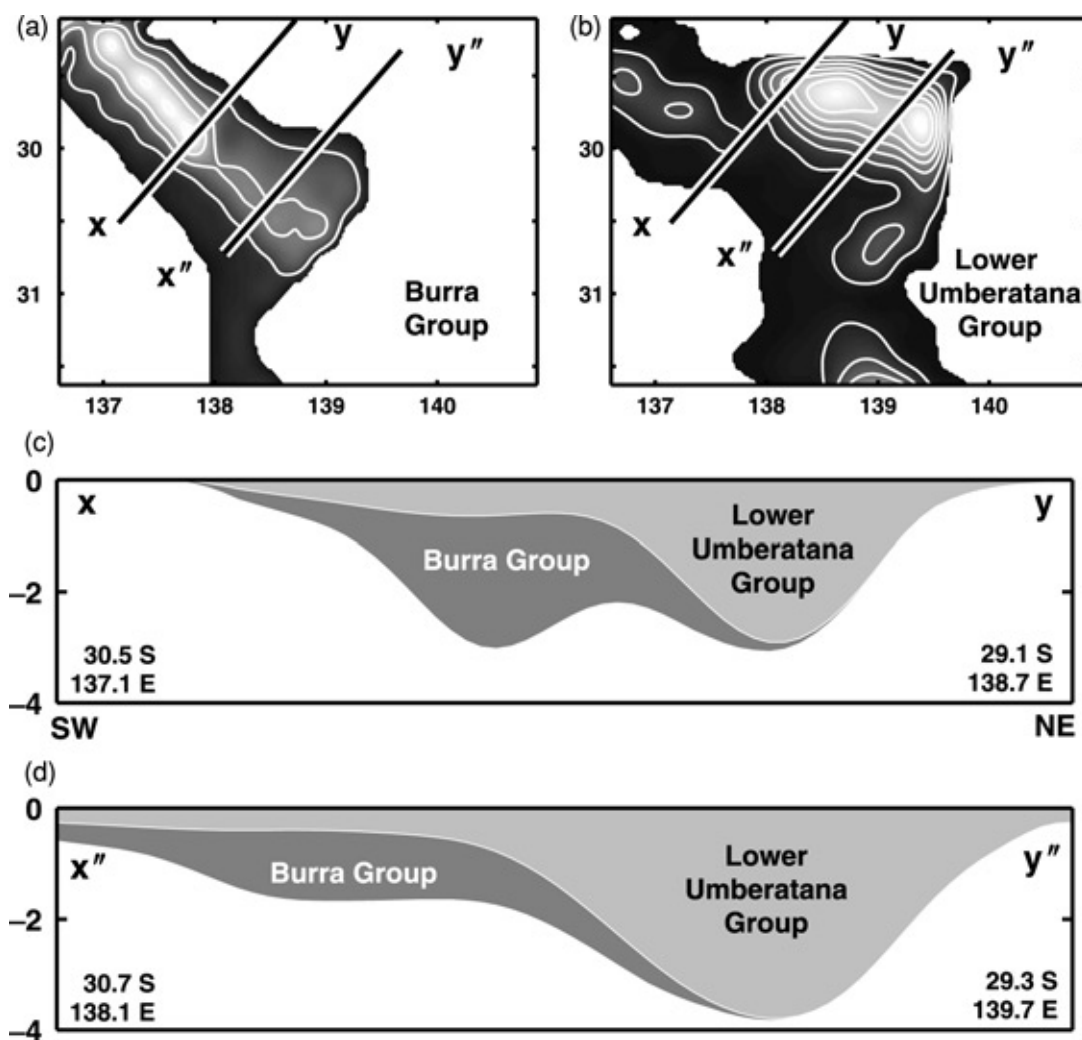


Fig. 1. Generalised isopach maps from Neoproterozoic successions in the northern Flinders Ranges, South Australia, showing a systematic shift in the locus of rifting during successive events associated with deposition of the Burra Group (Fig. 1a) and the lower Umberatana (Sturtian) Group (Fig. 1b), modified after Paul *et al.* (1999). The Umberatana Group depocentre is located at the margin of the Burra-aged rift basin, suggesting that the initial rifting has altered the mechanical structure of the lithosphere by the time that Umberatana-aged extension, some 50 Myr later. Figures 1c, d showing generalised profiles along section lines x-y and x''-y'', respectively.

thermal transients associated with advection of material during the deformation (Ter Voorde & Bertotti, 1994). Such transients can lead to short-term strength changes opposite in sign to the long-term strength changes that follow the dissipation of the thermal transients (e.g. Braun, 1992). This contribution focuses on the long-term strength changes, with ‘long-term’ used to signify a sufficient time interval since the initiating deformation that the thermal transients induced by the deformation have essentially dissipated (i.e. greater than about 50 Myr).

In addition to the potential for long-term changes in the gross-compositional structure of the continental lithosphere, significant changes in the distribution of heat producing elements (HPE’s) can be effected by deformation, especially when it is linked to surface processes (erosion, sedimentation) that act to restore the long-term surface elevation. Changes in the amount and depth of HPE’s associated with basin formation can lead to long-term changes in the thermal structure of the lithosphere (e.g. Sandiford, 1999). Because the mechanical strength of the lithosphere depends on its thermal state, the long-term mechanical consequences of rifting will be sensitive to any long-term changes in thermal regime. Such changes must inevitably result from changes in the distribution of the thermal properties (i.e. heat production, thermal conductivity) due to the rifting and the associated filling of the accommodation space. In the following section we evaluate the long-term thermal consequences of redistribution of heat production expected to result from rifting, with the specific aim of showing that rifting need not necessarily lead to significant long-term lithospheric strengthening. The work advances that of Sandiford (1999) in providing a new formalism for understanding the long-term thermal consequences of HPE redistribution associated with lithospheric deformation, and by exploring the thermal consequences of the 2D geometry of rift basins where lateral heat flow may significantly affect the steady-state thermal regime in the long term.

BACKGROUND

As noted above, crustal attenuation during rifting is expected to lead to long-term shallowing of the Moho, even in the case where the accommodation space resulting from attenuation is filled with sediment. For sediment-filled basins, the shallowing of the Moho can be related to the contrast between the densities of the basin filling sediment and the deep crust. Ignoring the contribution due to long-term changes in the thermal structure of the lithosphere, the total sediment-filled subsidence in a locally compensated basin is expected to scale as:

$$z_s \approx \frac{z_c(\beta - 1)}{\beta(\rho' + 1)} \quad (1)$$

In Eq. (1), β is a measure of the extent of crustal attenuation (e.g. McKenzie, 1978), z_c is the initial Moho depth, and ρ' is a measure of the ratio of the density

contrast between the crust and basin and mantle and crust, respectively.

$$\rho' = \frac{\rho_c - \rho_s}{\rho_m - \rho_c} \quad (2)$$

where ρ_c is the characteristic density of the crust, ρ_m is the characteristic density of the mantle and ρ_s is the characteristic density of the sediment fill. Note that ρ' also provides a measure of the ratio of long-term shallowing of the Moho to the thickness of sediment fill. The value of ρ' will vary depending on the nature of the sediment fill and is typically of the order of 0.6–0.7 implying that the long-term shallowing of the mantle is about 2/3 the thickness of the sediment-fill when the accommodation is totally filled.

The long-term change of Moho temperature attributable to the shallowing is given by the product of the steady-state temperature gradient at the Moho (q_m/k) and the change in Moho depth (Δz_c):

$$\begin{aligned} \Delta T_{q_m} &= \frac{q_m \Delta z_c}{k} \\ &= \frac{(\beta - 1)(2 + \rho') q_m z_c}{k \beta (1 + \rho')} \end{aligned} \quad (3)$$

For characteristic values of mantle heat flow ($q_m \sim 20\text{--}30 \text{ mW m}^{-2}$) and thermal conductivity ($k \sim 3 \text{ W m}^{-1} \text{ K}^{-1}$) the long-term Moho cooling is about $8\text{--}10^\circ\text{C}$ per kilometre of shallowing or $5\text{--}7^\circ\text{C}$ per kilometre of basin-fill. Greater cooling will occur when the accommodation is only partly filled because, for a given stretch, there will be greater Moho shallowing.

The factors that control the strength of the lithosphere are only poorly understood. Nevertheless, many workers believe that much of its strength resides in the upper-most mantle, where strength is likely to be limited by temperature activated creep processes. Consequently, the temperature of the Moho may provide a useful proxy for lithospheric strength (e.g. Brace & Kohlstedt, 1980; Sonder & England, 1986). If so, the long-term Moho cooling ($\sim 50^\circ\text{C}$) predicted to follow the formation of deep (5–10 km) rift basins would be expected to result in significant increases in lithospheric strength. Indeed, thermally modulated strength increases have been suggested as a principle control on the long-term mechanics of rift basins (e.g. England, 1983). Braun (1992) has termed this long-term strengthening as ‘mantle healing’ and demonstrated that it may provide a logical cause for the spatial separation of the locus of successive rifting events observed in some basins.

THERMAL CONSEQUENCES OF HEAT PRODUCTION REDISTRIBUTION

This section outlines a simple formalism that allows the evaluation of some important long-term thermal consequences of the redistribution of HPE’s that must inevitably accompany the formation of rift basins. HPE’s

are redistributed during rifting as a consequence of the crustal attenuation, due to the burial of the attenuated crust beneath the basin-fill, and due to the HPE's contained within the basin-fill. While attenuation of the pre-existing crust leads to long-term Moho cooling, burial of the heat production in the attenuated crust beneath the basin-fill leads to Moho heating. Below we explore how this competition between the attenuation and burial is resolved for thermal parameters appropriate to typical continental crust. We begin by assuming that lithospheric heat production is contained entirely within the crust, and that lateral variations in heat production are insignificant. The first assumption is justified by analyses of peridotite showing that concentrations of heat producing elements in mantle rocks are typically an order of magnitude lower than in crustal rocks (Haenel *et al.*, 1988). The second assumption allows the problem to be treated in terms of the vertical conduction of heat. While this is clearly a gross simplification, it provides a useful starting point since vertical temperature gradients (typically greater than $10^{\circ}\text{C km}^{-1}$) are invariably more than an order of magnitude larger than lateral temperature gradients (typically less than $1^{\circ}\text{C km}^{-1}$) once thermal transients associated with deformation have dissipated. This assumption restricts our attention to basins with lateral dimensions significantly greater than the thickness of the lithosphere. The consequences of lateral heat conduction specific to spatially restricted basin development are explored later in this paper.

For any heat production distribution $H(z)$ subject to the conditions above, the temperature field relative to the surface temperature is given by

$$T(z) = \frac{1}{k} \int_0^z \left\{ \int_{z'}^{z_1} H(z'') dz'' \right\} dz' + \frac{q_m z}{k} \quad (4)$$

where the first term on the right is the contribution of lithospheric heat sources and the second term is the contribution due to the heat flow applied to the base of the lithosphere (depth z_1).

The first term on the right in Eq. (4) depends only on the amount and distribution of heat sources and suggests an analysis in terms of parameters that do not require any a priori assumptions about the distribution. Two such parameters are q_c and h , defined as follows (see Sandiford & McLaren (2002) for further details):

$$q_c = \int_0^{z_1} H(z) dz \quad (5)$$

$$h = \frac{1}{q_c} \int_0^{z_1} (H(z) z) dz \quad (6)$$

While the parameter q_c strictly provides a measure of the total heat contributed by radiogenic sources in the lithosphere, we consider the case where the HPE's are essentially restricted to the crust, and the domain of integration can be limited to the crust (i.e. z_1 can be

replaced with z_c). Thus, in the 1D approximation, q_c represents the contribution of crustal heat generation to the surface heat flow. The parameter h provides a measure of the characteristic depth of the crustal heat production distribution (Fig. 2, Appendix).

Assuming temperature independent conductivity, the contribution of HPE's to the temperature of the Moho, T_{Moho} , is (Fig. 2):

$$T'_{q_c} = \frac{q_c h}{k} \quad (7)$$

with the Moho temperature (relative to the surface of the lithosphere) given by

$$\begin{aligned} T_{\text{Moho}} &= T'_{q_c} + T_{q_m} \\ &= \frac{q_c h}{k} + \frac{q_m z_c}{k} \end{aligned} \quad (8)$$

Equation (8) provides some useful insights into the factors controlling the Moho temperature. Analysis of surface heat flow data suggests that $\sim 1/2$ – $2/3$ of the surface heat flow can be attributed to crustal sources, with the remainder due to heat flow from beneath the lithosphere (e.g. McLennan & Taylor, 1996; Sandiford & McLaren, 2002). The same data implies that heat sources are concentrated in the upper $1/2$ of the crust (see further discussion below). Bearing in mind these parameters, approximately $1/4$ – $1/3$ of T_{Moho} is attributable to crustal radiogenic sources, with the remainder due to mantle heat flow. The dependence of T_{Moho} on h and q_c implies that changes in heat production distribution attendant with rifting will affect the long-term thermal and mechanical structure of the crust.

In order to explore the long-term thermal consequences of the redistribution of heat sources due to rifting we assume (1) rifting acts to homogeneously thin the crust, and (2) following rifting lithospheric cooling proceeds to restore the pre-rift mantle heat flow, q_m . With these assumptions the long-term changes in T_{Moho} are attributable to (1) changes in h and q_c and (2) changes in the depth of the Moho (i.e. Eq. (3)).

The assumption of homogeneous stretching implies that following rifting the total heat production contributed by pre-existing crustal heat sources is q_c/β while the attenuated heat production, now buried beneath the basin-fill, has a characteristic depth $z_s + h/\beta$. Following rifting by a factor β the long-term change in Moho temperature due to the redistribution of pre-existing crustal heat sources is

$$\begin{aligned} \Delta T'_{q_c} &= \frac{(q_c/\beta)(z_s + h/\beta)}{k} - \frac{q_c h}{k} \\ &= q_c \frac{(h - h\beta^2 + \beta z_s)}{k\beta^2} \\ &= -q_c \left(\frac{(\beta - 1)(h(1 + \beta)(1 + \rho') - z_c)}{k\beta^2(1 + \rho')} \right) \end{aligned} \quad (9)$$

The attenuation of heat production will naturally lead to a reduction in T_{Moho} because $q_c/\beta < q_c$. In contrast, the change in depth of the heat production may lead to either

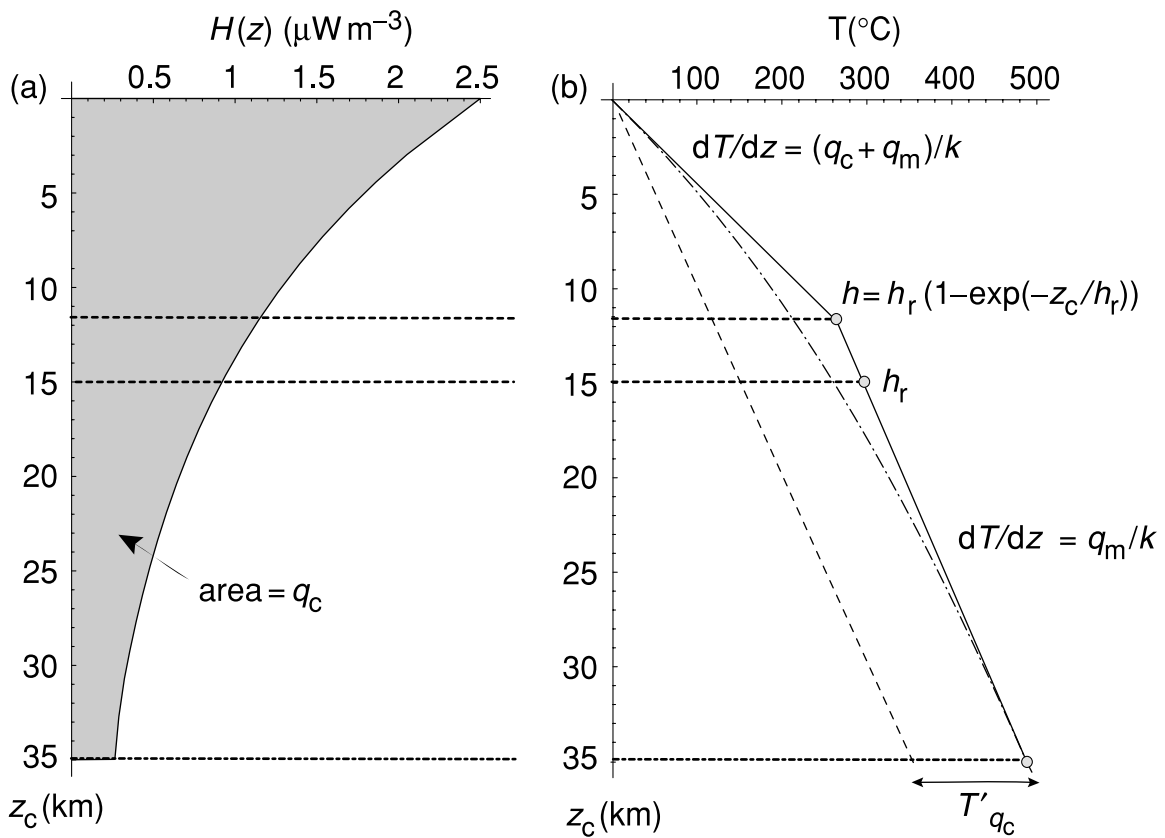


Fig. 2. Illustration of the connection between the effective depth of the crustal heat production h , the vertically integrated complement of HPEs, termed q_c (Fig. 2a), and the perturbation of the geotherm due to the heat production, T'_{q_c} (Fig. 2b). The heat production is modelled as an exponentially reducing function of depth (characterised by an e-fold length, h) terminating at the Moho (z_c). The maximum value of T'_{q_c} , $T'_{q'_c}$, occurs at the base of the heat-producing layer (i.e. z_c) and is given by hq_c/k . For crustal heat production field consisting of a layer of uniform heat production of thickness h , $h = h/2$.

a reduction or an increase in T_{Moho} , depending primarily on the values of ρ' and h . Figs 3–10 show the effect of the various parameters on the long-term thermal consequences of rifting in terms of both $\Delta T'_{q_c}$ and ΔT_{Moho} .

With the proviso that all accommodation is filled with sediment, rifting will result in an increase in T'_{q_c} (i.e. $\Delta T'_{q_c} > 0$) provided that

$$h < \frac{z_c}{(\beta + 1)(1 + \rho')} \quad (10)$$

For the parameter values listed in Table 1, this yields $h < 8$ km when the basin-fill contains no heat production (Figs 3a and 4a) or $h < 10$ km when the basin-fill heat production is $1.5 \mu\text{W m}^{-3}$ (Fig. 4b). As implicit in the Eq. (10), the vertical distribution of the heat sources in the pre-existing crust is critical to the long-term thermal response of the lithosphere of rifting. A completely undifferentiated crust, with uniform heat production throughout ($h \sim 15$ km, see Appendix Section) yields substantial ($> 40 ^{\circ}\text{C}$) long-term reductions in both T'_{q_c} and T_{Moho} even when the basin-fill contains significant heat production (Fig. 4). An important conclusion highlighted by Figs 3 and 4 is that the long-term thermal consequences

of rifting are far more sensitive to vertical distribution of heat production in the crust than to the absolute amount of heat production, with an increase in h from 5 to 10 km resulting in a change in $\Delta T'_{q_c}$ of $\sim 40 ^{\circ}\text{C}$ for $\beta = 1.5$.

A constraint on the range of values of h appropriate to continental crust is provided by an analysis of surface heat flow and heat production data (e.g. Lachenbruch, 1968; Roy *et al.*, 1968). Plots of surface heat flow as a function of heat production commonly define quasi-linear arrays within individual heat flow provinces, with regression slopes typically in the range 7–12 km and intercepts of about 30 mW m^{-2} . This slope, h , has commonly been interpreted as the characteristic vertical length-scale for the HPE distribution while the intercept, which defines the reduced heat flow, q_r , is interpreted as the non-radiogenic component of the surface heat flow (e.g. Lachenbruch, 1968). For a distribution that reduced exponentially with depth h is often equated with the depth at which the heat production is $1/e$ (the e-fold length) of its surface value. Alternatively it is equated with the thickness of a slab of approximately uniform thickness, which contains all the heat production variation responsible for the observed variation in the surface heat flow field. However, the inevitable lateral heat flow induced by the spatial

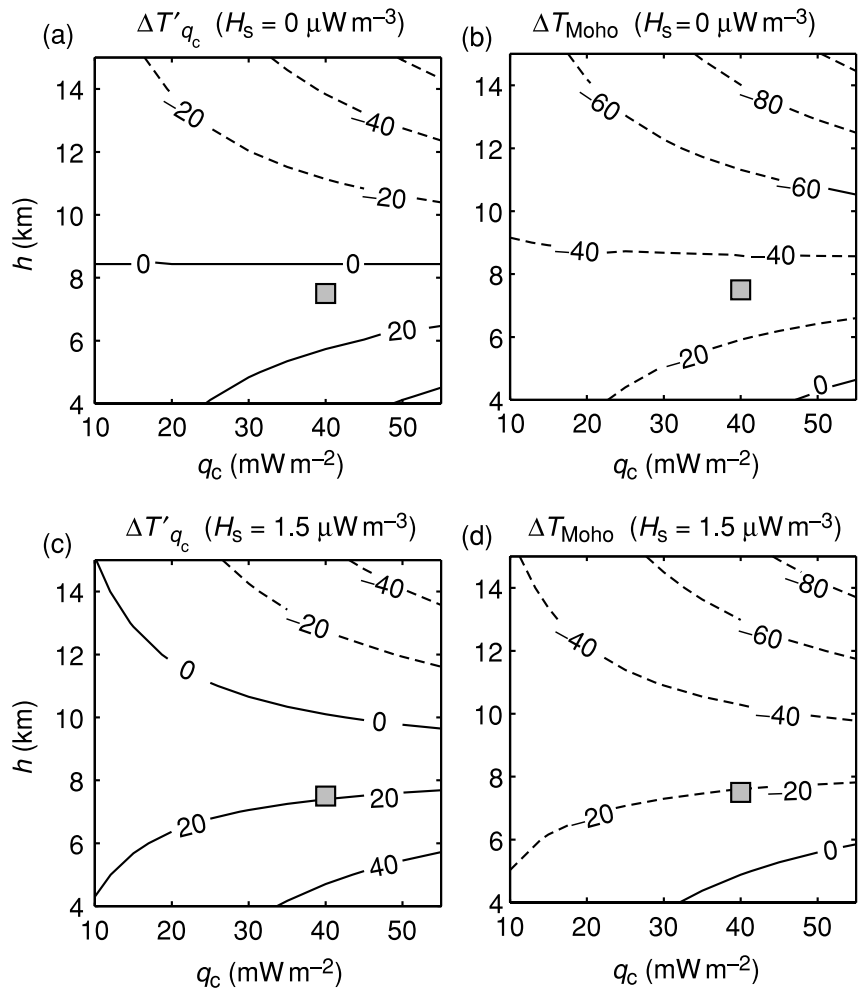


Fig. 3. Illustration of the dependence of $\Delta T'_{q_c}$ and ΔT_{Moho} on q_c and h for a rifting event $\beta = 1.5$ when the accommodation space entirely filled with sediment ($\lambda = 1$). Figures 3a,b show the case where the basin-fill contains no heat production ($H_s = 0$ – see Eq. (9)) while Figs 3c,d apply for basin-fill heat production of $1.5 \mu\text{W m}^{-3}$. Squares show the position of the reference lithosphere defined by the default parameter values as listed in Table 1. The default parameter range yields a small positive $\Delta T'_{q_c}$ (+5 to +20 °C) and negative ΔT_{q_m} (-35 to -20 °C).

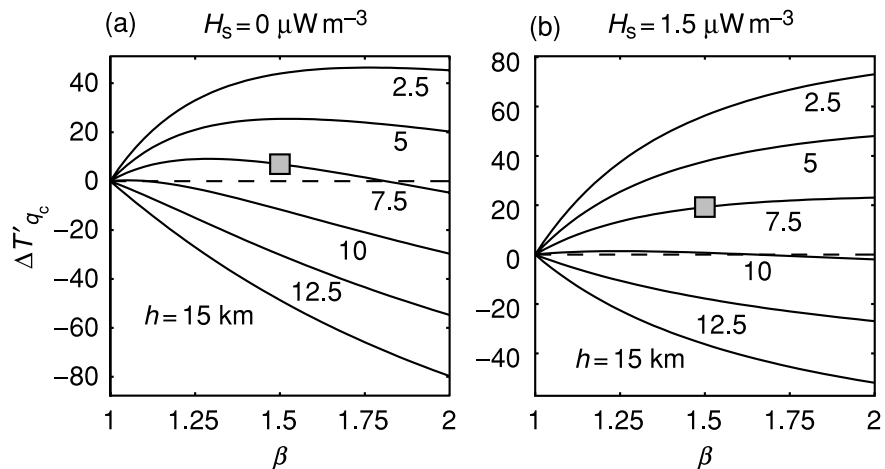


Fig. 4. Illustration of the dependence of $\Delta T'_{q_c}$ on h and β . Figure 4a shows the case where the basin-fill contains no heat production ($H_s = 0$) while Fig. 4b applies for basin-fill heat production of $1.5 \mu\text{W m}^{-3}$. Squares show the position of the reference lithosphere. All other parameter values are default values listed in Table 1.

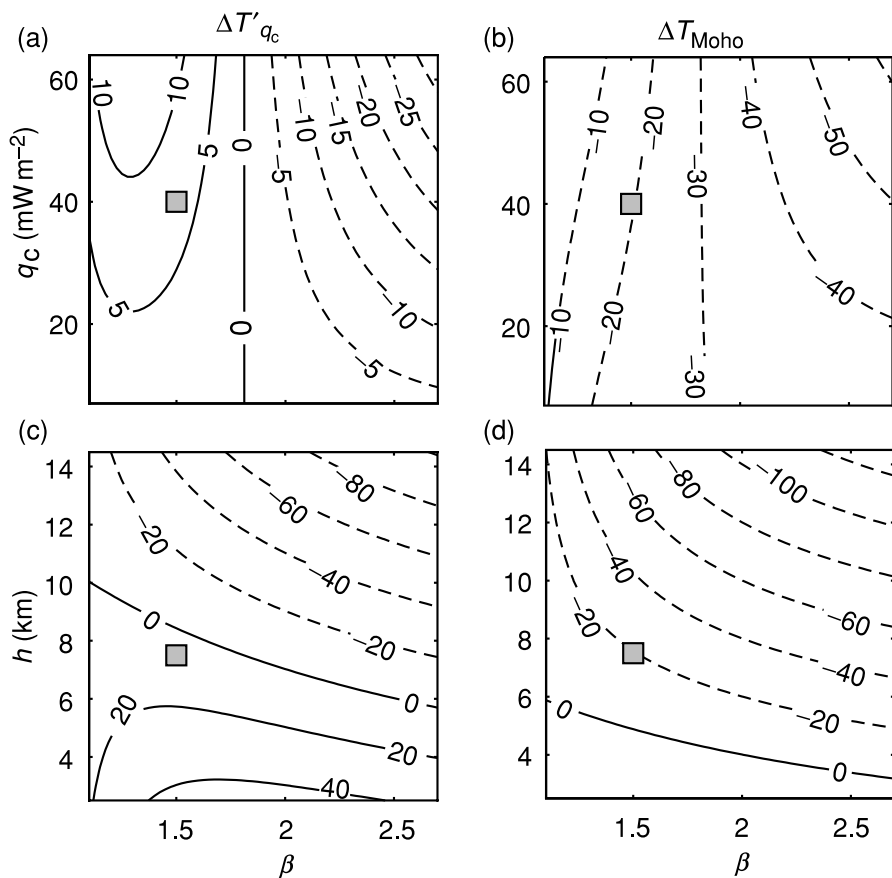


Fig. 5. Illustration of dependence of $\Delta T'_{q_c}$ and ΔT_{Moho} on q_c (Figs 5a, b) and h (Figs 5c, d) as a function of β . Squares show the position of the reference lithosphere defined by default parameter values as listed in Table 1.

Table 1. Summary of symbols used in text, default parameter values and ranges used in calculations.

| Symbol | Default value | Range |
|---|-------------------------------------|-----------|
| q_c – Radiogenic heat flow contribution | 40 mW m^{-2} | 20–50 |
| q_m – Non-radiogenic heat flow contribution | 25 mW m^{-2} | 15–35 |
| q' – Ratio of radiogenic to non-radiogenic heatflow contributions (q_c/q_m) | q_c/q_m | 0.4–1.6 |
| h – Effective depth of heat production | 7.5 km | 2–12 |
| H_s – Sediment heat production | $1.5 \mu\text{W m}^{-3}$ | 0–2.5 |
| H_{uc} – Upper crustal heat production | $3 \mu\text{W m}^{-3}$ | 1.5–7 |
| z_s – Basin thickness | 6 km | 2.5–12 |
| β – Stretching factor | 1.5 | |
| ρ' – Density parameterisation $(\rho_c - \rho_s)/(\rho_m - \rho_c)$ | 0.66 | 0.35–0.9 |
| ρ_c – Density of crust | 2750 kg m^{-3} | |
| ρ_s – Density of basin-fill | 2350 kg m^{-3} | |
| ρ_m – Density of mantle | 3350 kg m^{-3} | 2150–2550 |
| z_c – Reference crustal thickness | 35 km | |
| k_s – Thermal conductivity of basin-fill | $3 \text{ W m}^{-1} \text{ K}^{-1}$ | 1.5–3.5 |
| k_c – Thermal conductivity of crust | $3 \text{ W m}^{-1} \text{ K}^{-1}$ | |
| λ – Basin-fill accommodation factor | 1 | |
| $x_{1/2}$ – Basin half width | | 20–150 |
| x_r – Basin ramp width | | 4–150 |
| x' – Ratio of ramp width to basin half width | 0.6 | 0.2–1 |

variations in crustal HPE parameters required to produce such arrays will always result in the shallowing of such arrays (England *et al.*, 1980; Jaupart, 1983; Nielsen, 1987). The slope therefore provides only a lower bound on the characteristic length-scale of the HPE distribution, while the intercept provides an upper bound on the non-radiogenic component of the heat flow. The effects of lateral heat flow on the slope of such regressions conceivably yields underestimates of the true length-scales by as much as 30% (Jaupart, 1983; Sandiford & McLaren, 2002) as well as overestimates in the non-radiogenic component of the heat flow. However, as shown in the Appendix, h will typically be lower than the h by an amount that is sensitive to the way the HPE distribution varies with depth. For HPE distributions showing inverse exponential dependence on depth (e.g. Roy *et al.*, 1968), h is expected to be ~80% of h , for e-fold lengths of ~15 km. For a distribution consisting of a slab of approximately uniform heat production, h is approximately 50% of the slab thickness. These considerations suggest that the characteristic values of h for continental crust are likely in the range 5–12 km. A default value of h of 7.5 km is used in the calculations summarised below.

Figure 3a shows that for the default values shown in Table 1 appropriate to a typical continental crust, $\Delta T'_{q_c}$ is about +7 °C, taking no account of additional heat production contributed by the basin-fill. Of course, changes in the Moho temperature (ΔT_{Moho}) will also reflect the shallowing of the mantle, and the additional heat production contributed by the basin-fill (as well as any differences in thermal conductivity between the basin-fill and the underlying crust). Figure 3b shows that cooling due to Moho shallowing significantly outweighs $\Delta T'_{q_c}$ for almost all of $h-q_c$ space, leading to long-term reduction in T_{Moho} of ~35 °C when there is no heat production in the sediment fill.

The contribution of basin-fill heat production to the temperatures at depth beneath the base of the basin can be approximated by:

$$\Delta T_{H_s} = \frac{\langle H_s \rangle z_s^2}{2k} \quad (11)$$

where $\langle H_s \rangle$ is the mean heat production of the basin-fill. Figures 3c, d show the predicted changes in $\Delta T'_{q_c}$ and ΔT_{Moho} for the basin-fill heat production of 1.5 $\mu\text{W m}^{-3}$. Again, the anticipated cooling due to Moho shallowing (i.e. ΔT_{q_m}) is greater than the heating due to burial of the existing heat production (i.e. $\Delta T'_{q_c}$) for all but high- q_c , low- h configurations. For the default parameters chosen here to characterise typical continental crust (Table 1), the predicted long-term Moho cooling is ~20 °C, for a $\beta = 1.5$.

There is a large range in the plausible values of the relevant crustal and basin fill thermal parameters (Table 1), precluding a simple analysis of the potential long-term thermal consequences of rifting. The approach adopted here to illustrate the effect of the plausible parameter range utilises a Monte Carlo method, following Hansen & Nielsen (2002), with calculations performed

on sets of uniformly distributed random combinations of the relevant parameters. The parameter ranges are as listed in Table 1. $\Delta T'_{q_c}$ and ΔT_{Moho} have been estimated for combinations of the main parameters (Figs 6–8), initially neglecting the possibility of thermal conductivity contrasts between the basin-fill and underlying crust.

Figures 6–8 show that, in addition to h , the long-term thermal response to rifting is particularly sensitive to the extent of rifting, and the density and the heat production character of the basin-fill. Increasing the relative density of the fill (i.e. a reduction in ρ') and its heat production increases both T'_{q_c} and T_{Moho} because, for a given stretching factor, there is (1) a greater thickness of basin-fill leading to an increase in $\Delta T'_{q_c}$ and (2) less shallowing of the Moho leading to a decrease in ΔT_{q_m} . ΔT_{Moho} is also dependent on q_m (decreasing with q_m) while $\Delta T'_{q_c}$ and ΔT_{Moho} are both dependent on H_{uc} (increasing with H_{uc} , since the implemented parameterisation couples H_{uc} , h and q_c via the relation $q_c = 2hH_{uc}$). In the absence of conductivity contrasts between the basin-fill and the underlying crust, the parameter space appropriate to long-term Moho heating is small (Figs 7 and 8b), largely restricted to very low values of h and/or ρ' , relative to the default values. In contrast, the parameter space to long-term increases in T'_{q_c} is large (Fig. 6), with in excess of 70% of the modelled parameter sets showing $\Delta T'_{q_c} > 0$ (Fig. 8a). Provided that the accommodation is filled, the implication is that rifting should normally be expected to lead to long-term increases in average crustal thermal gradients, even in the absence of conductivity contrasts between the basin-fill and the underlying crust. The mean difference between $\Delta T'_{q_c}$ and ΔT_{Moho} is 36°, a value that largely reflects, and is sensitive to, the modelled range in q_m .

The arguments presented above are mostly subject to the proviso that the accommodation created by rifting is filled entirely by sediment. Moreover, we have assessed the accommodation using a local isostatic basis, implying no long-term flexural strength of the lithosphere. For lithosphere with long-term flexural strength, the patterns of accommodation generation are more complicated, and require a higher level of sophistication in the analysis that tends to obscure the points we have been interested in exploring here. Nevertheless, a qualitative guide to the effects of flexural rigidity may be appreciated with reference to partial filling, since the thickness of the accommodation scales inversely with the flexural rigidity. Partial filling ($\lambda < 1$) has the consequences that (1) the Moho shows greater long-term shallowing and (2) the pre-existing heat production remains shallower. Both factors cause a lowering of both $\Delta T'_{q_c}$ and ΔT_{Moho} relative to the filled-basin scenario (Fig. 9).

EFFECT OF THERMAL CONDUCTIVITY CONTRASTS

Thermal conductivity contrasts between the basin-fill and the pre-existing crust are to be expected, because the thermal conductivity of basin-filling sediments is generally

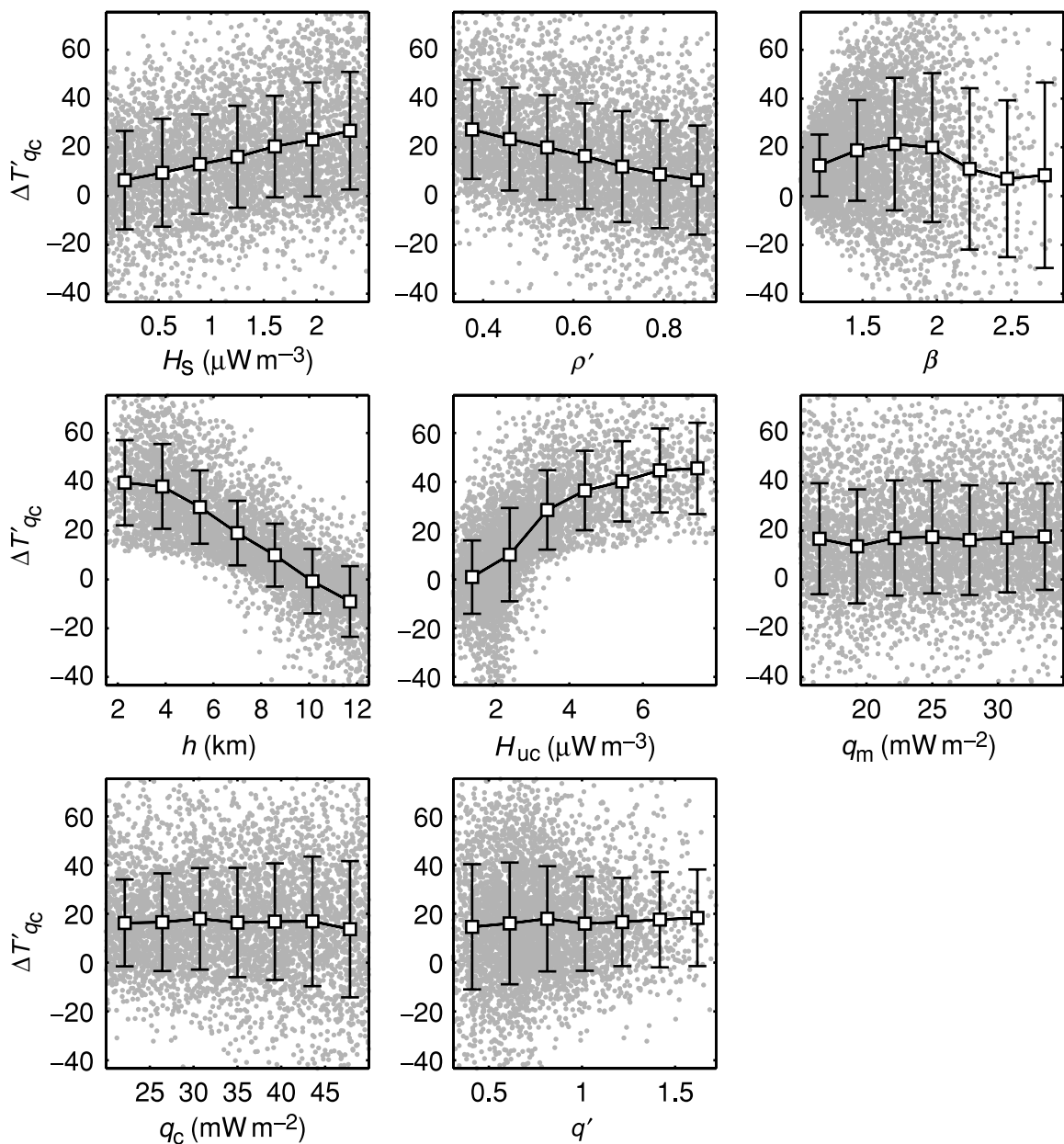


Fig. 6. Illustration of dependence of $\Delta T'_{qc}$ on the relevant parameter ranges for crust and basin fill. Dots show the location of ~ 4600 random parameter sets, within the ranges listed in Table 1, with the data fitted by the mean and standard deviation of seven discrete bins.

lower than that of metamorphic and igneous rocks that comprise the bulk of the crust (e.g. Pereira *et al.*, 1986). Following Sandiford (1999), the impact of such a conductivity contrast on the temperature field in the deep crust can be expressed as

$$\Delta T_{k_s} = z_s \left(q_m + \frac{q_c}{\beta} \right) \left(\frac{1}{\langle k_s \rangle} - \frac{1}{\langle k_c \rangle} \right) \quad (12)$$

where $\langle k_s \rangle$ is the characteristic thermal conductivity of the basin fill, and $\langle k_c \rangle$ is the characteristic value of the crust.

Figure 10 shows the impact of thermal conductivity contrasts using the Monte Carlo approach outlined above, and highlights the fact that only relatively minor reductions in the conductivity of the basin fill relative to the underlying crust are needed for a long-term increase

in T_{Moho} beneath the basin. For a crustal conductivity of $3 \text{ W m}^{-1} \text{ K}^{-1}$, the mean ΔT_{Moho} exceeds 0 when the conductivity of the basin-fill is less than $2.5 \text{ W m}^{-1} \text{ K}^{-1}$ (Fig. 10b). When the basin-fill includes a significant proportion of shale, the thermal conductivity differential with the underlying crust is likely to exceed $0.5 \text{ W m}^{-1} \text{ K}^{-1}$ (e.g. Pereira *et al.*, 1986), raising the possibility that many basins naturally lead to an increase in T_{Moho} as well as T'_{qc} .

2D-EFFECTS IN CONFINED BASINS

The calculations summarised above show that in the absence of thermal conductivity contrasts between basin fill and the underlying crust, the most likely long-term

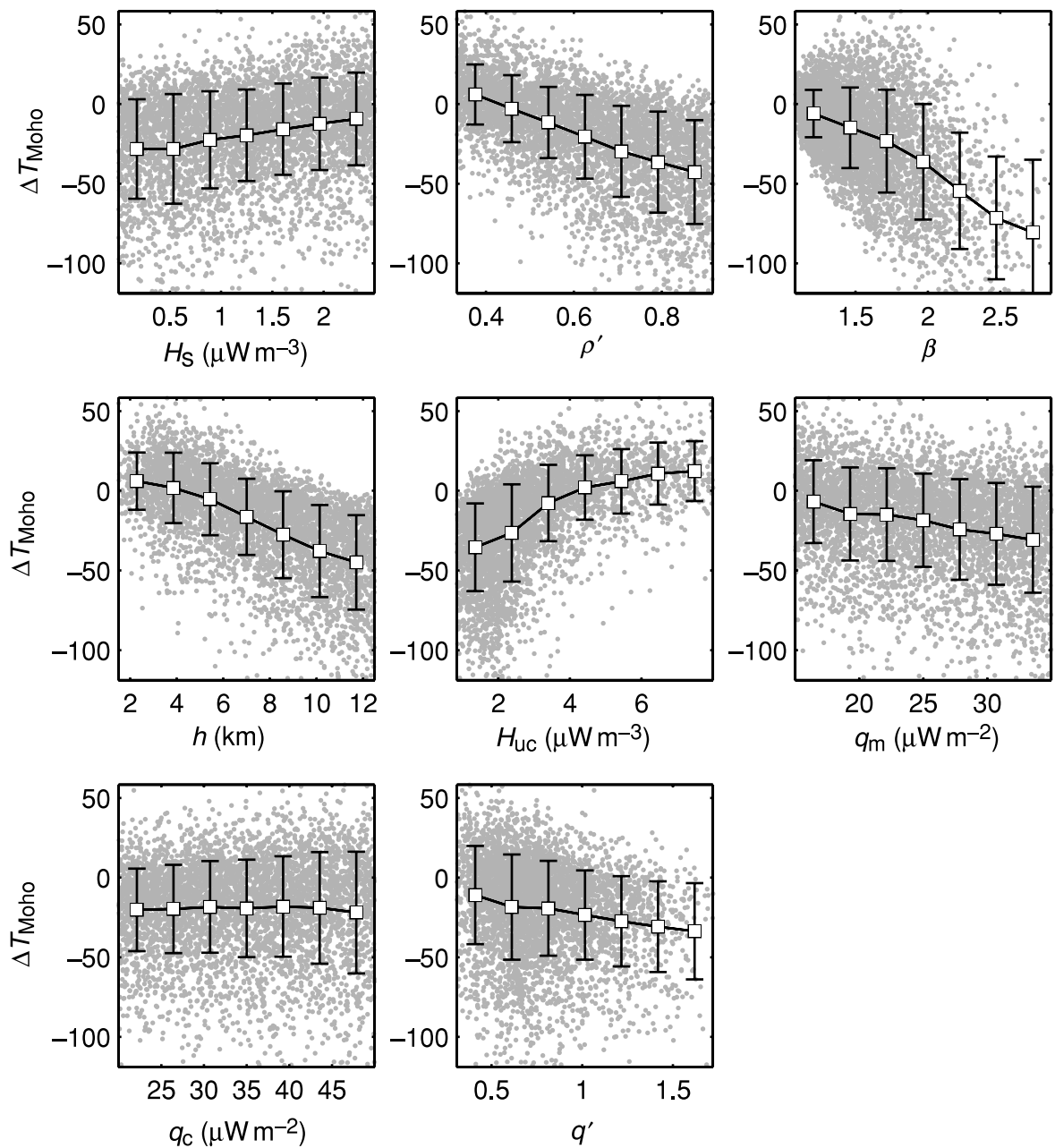


Fig. 7. Illustration of dependence of ΔT_{Moho} on relevant parameter ranges for crust and basin fill. Dots show the location of ~ 4600 random parameter sets, within the ranges listed in Table 1, with the data fitted by the mean and standard deviation of seven discrete bins.

thermal consequence of rift basin filling is to increase the average crustal thermal gradients, while simultaneously cooling the Moho. If the basin-fill has a substantially lower thermal conductivity than the underlying crust, as is likely when it contains an appreciable proportion of shale, basin formation is likely to lead to long-term increases in Moho temperature despite the Moho shallowing. An important consequence of this thermal structuring of the lithosphere is to induce long-term lateral heat flow from beneath confined basins of finite width towards their margins (Fig. 11). As pointed out by Hansen & Nielsen (2002) for narrow basins, the effect of the lateral heat flow is to enhance the Moho cooling (or reduce Moho heating) beneath the basin while

simultaneously increasing the Moho temperatures beneath the rift margins (Fig. 11b). Such thermal structuring may have potentially important consequences for the long-term strength distribution of rifted lithosphere. This section explores the role of lateral heat conduction, using a Monte Carlo approach inspired by Hansen & Nielsen, 2002), for our choice of parameterisation as outlined in Table 1.

The basic geometric model used in the finite element simulations (Fig. 11a) is characterised by a flat basin floor of half width $x_{1/2}$ and a margin characterised by a ramp of width x_r from fully extended crust to unextended crust. In the reference crust, heat production is contained within a slab of thickness z_{uc} . The initial value of h is

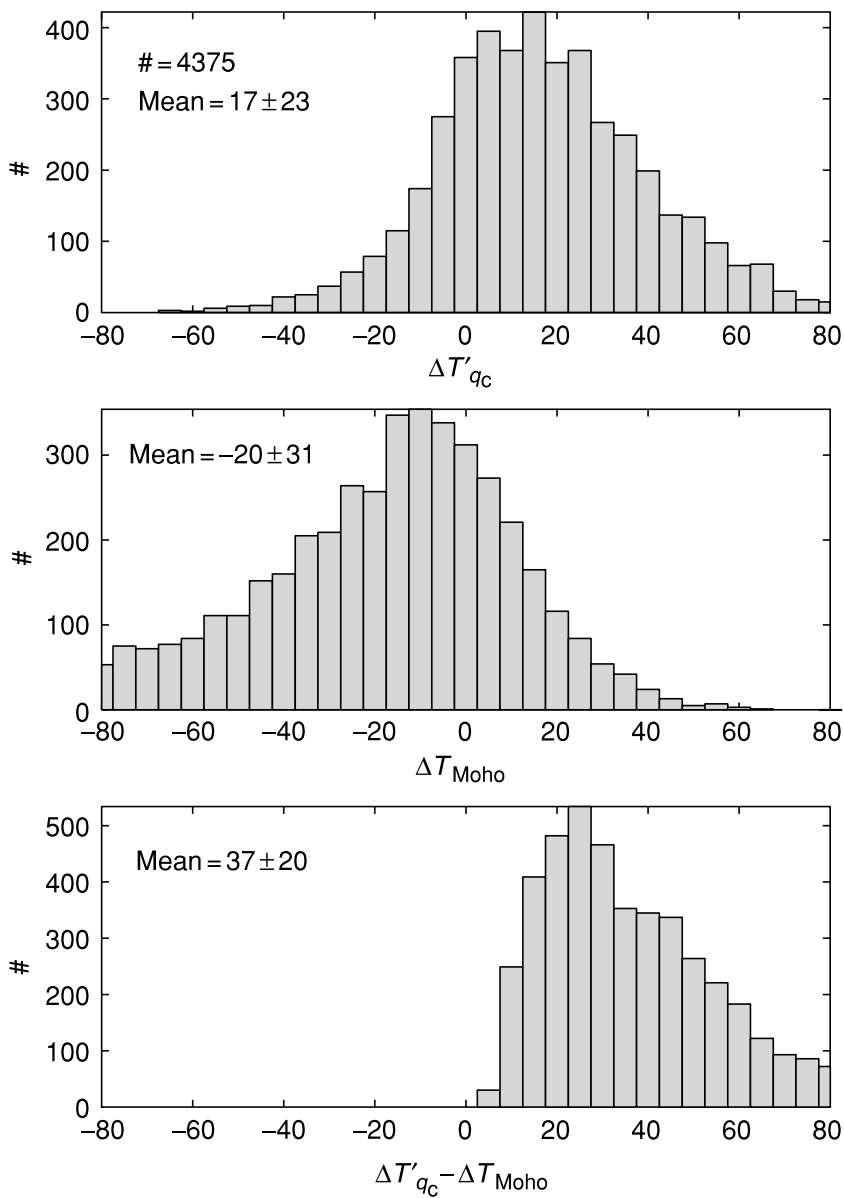


Fig. 8. Histogram representation of calculations summarised in Figs 6 and 7, showing that, in the 1D-limit, the likely long-term thermal response of basin formation is to increase T'_{qc} (Fig. 8a) but decrease T_{Moho} (Fig. 8b).

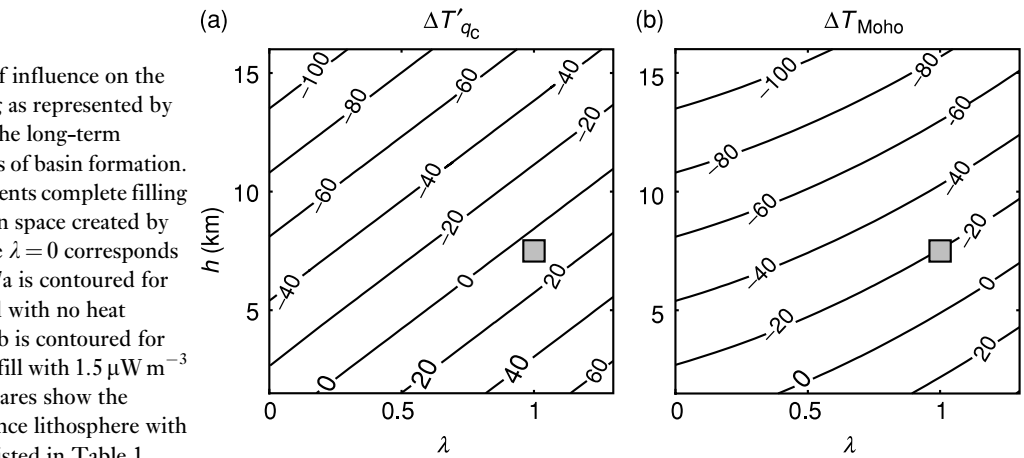


Fig. 9. Illustration of influence on the extent of basin-filling as represented by the parameter λ , on the long-term thermal consequences of basin formation. The case $\lambda = 1$ represents complete filling of the accommodation space created by rifting, while the case $\lambda = 0$ corresponds to no filling. Figure 7a is contoured for $\Delta T'_{qc}$ with a basin-fill with no heat production. Figure 7b is contoured for ΔT_{Moho} with a basin-fill with $1.5 \mu\text{W m}^{-3}$ heat production. Squares show the position of the reference lithosphere with parameter values as listed in Table 1.

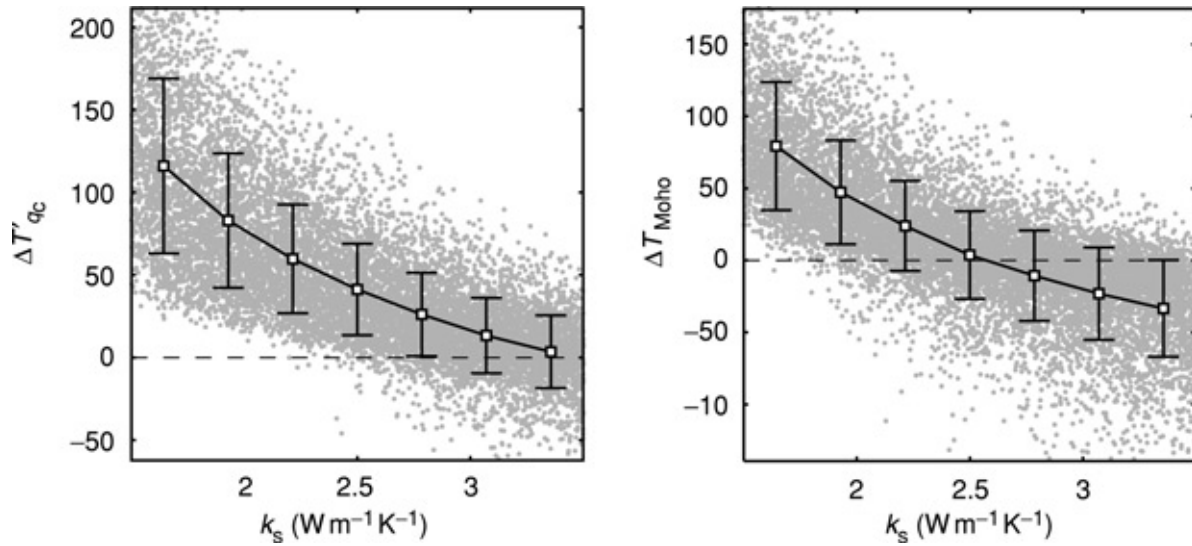


Fig. 10. Illustration of the dependence of $\Delta T'_{qc}$ and ΔT_{Moho} on conductivity of basin fill, for ~ 8000 sets of randomly chosen parameters in the range listed in Table 1. Conductivity of the crust is $3 \text{ W m}^{-1} \text{ K}^{-1}$.

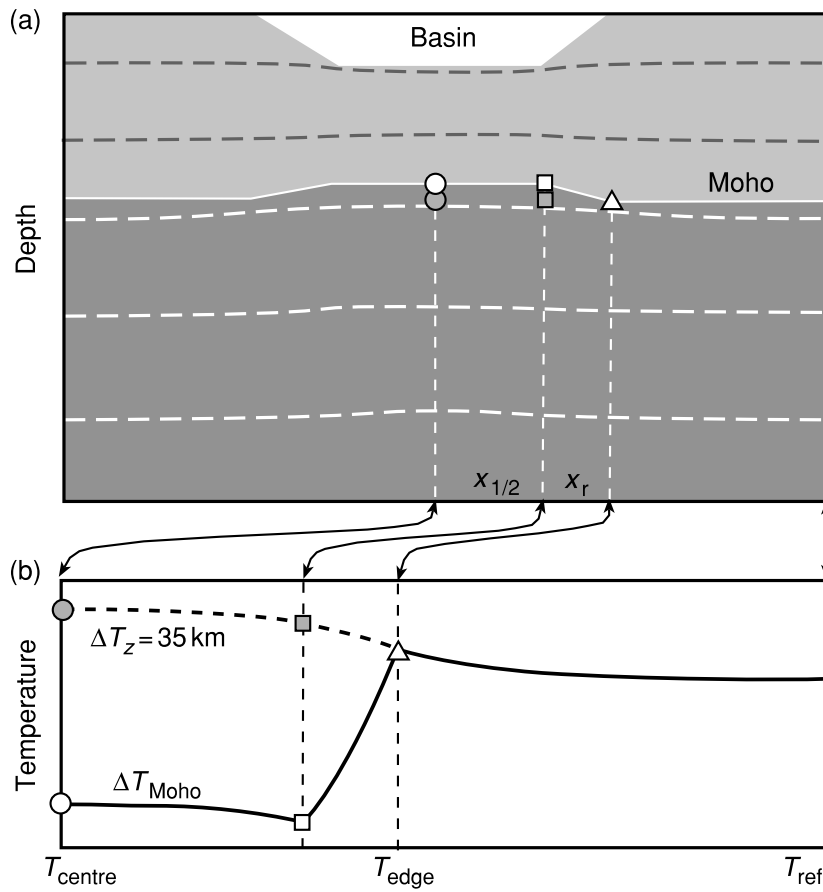


Fig. 11. Schematic illustration of rift basin used to explore the 2D-effects of rift basin geometry. In the long term basin formation shallows and cools the Moho, whilst steepening the geotherm beneath the basin centre (Fig. 8a). Consequently lateral heat flow away from the basin tends to heat the Moho under the rift flanks (Fig. 8b). Basin width is characterised by the half width of the basin floor ($x_{1/2}$) and the ramp width (x_r).

therefore $z_{uc}/2$ (see Appendix Section). The Monte Carlo simulation involved $\sim 10\,000$ solutions to the 2D heat conduction equation for a randomly distributed set of thermal parameters in the range listed in Table 1. The results are presented (Figs 12–17) in terms of the differences in Moho temperatures between the basin centre

and the initial or far field lithosphere ($T_{\text{centre}} - T_{\text{ref}}$), the basin margin and the far field ($T_{\text{edge}} - T_{\text{ref}}$) and the basin centre and basin margin ($T_{\text{centre}} - T_{\text{edge}}$).

Figure 12 shows the computed values of $T_{\text{centre}} - T_{\text{ref}}$, $T_{\text{edge}} - T_{\text{ref}}$, and $T_{\text{centre}} - T_{\text{edge}}$ as a function of basin width for default parameter set as listed in Table 1. The

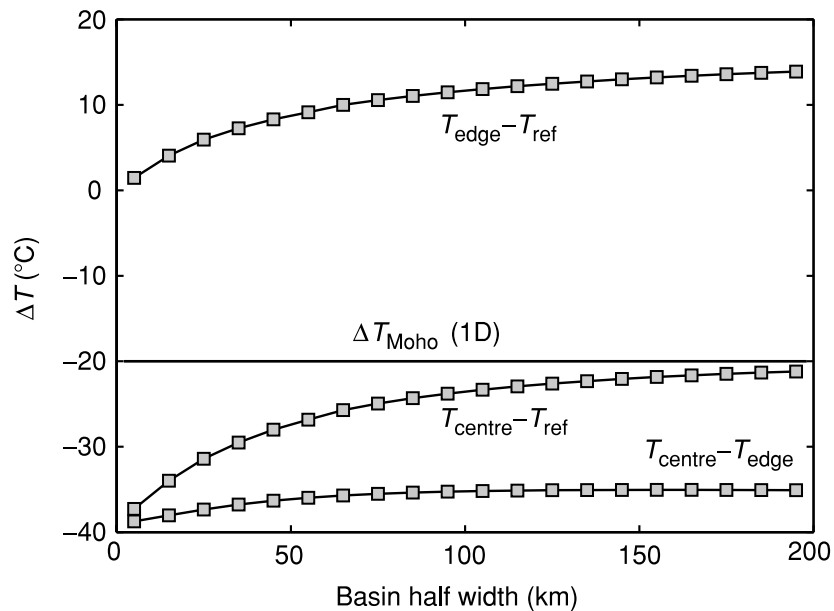


Fig. 12. Illustration of the influence of basin half width ($x_{1/2}$) on Moho temperatures. Ramp width is 60% of $x_{1/2}$.

parameter $T_{\text{centre}} - T_{\text{ref}}$ is the 2D-equivalent of ΔT_{Moho} , which for the modelled parameter set is -20°C while $\Delta T'_{qc}$ is 20°C . The effect of basin width is significant for $x_{1/2} < \sim 100\text{ km}$ and particularly dramatic when $x_{1/2} < \sim 50\text{ km}$.

Figures 13 and 14 show the calculated values of $T_{\text{centre}} - T_{\text{ref}}$, $T_{\text{edge}} - T_{\text{ref}}$ for each of the principal parameter ranges listed in Table 1. A summary of all results is shown in Fig. 15. In addition to basin width, the critical parameters affecting the long-term thermal response to rifting are the density and conductivity of the basin-fill, and the distribution of heat sources in the pre-existing crust. The magnitude of the mantle heat flow q_m plays only a minor role showing a weak inverse correlation with $T_{\text{centre}} - T_{\text{ref}}$. About 50% of the solutions showed long-term Moho heating beneath the basin (i.e. $T_{\text{centre}} - T_{\text{ref}} > 0$, Fig. 15a) while in excess of 90% showed long-term Moho heating beneath the basin margin (i.e. $T_{\text{edge}} - T_{\text{ref}} > 0$, Fig. 15b), with the mean Moho temperature rise beneath the basin margin of $\sim 13^{\circ}\text{C}$. A maxima in the basin margin Moho heating occurs at basin half widths of $\sim 50\text{ km}$ (Fig. 14). In about 30% of the modelled parameter sets, characterised by a basin-fill with low thermal conductivity ($k_s < 2.25\text{ W m}^{-1}\text{ K}^{-1}$) and relatively high density ($\rho' < 0.55$), the hottest Moho temperatures occur beneath the centre of the basin (i.e. $T_{\text{centre}} - T_{\text{edge}} > 0$, Fig. 15c). Such low conductivities require a high-proportion of shale, and consequently the basin-fill densities are also likely to be low. Therefore, the combination of basin-fill parameters that yield Moho temperature maxima beneath the basin centre is unlikely to occur in natural basins. When there is no conductivity contrast between basin-fill and the underlying crust, only a few percent of configurations lead to long-term Moho heating beneath the basin centre (Fig. 16a), with an almost equal probability of Moho heating and cooling beneath the basin margin (Fig. 16b).

Figure 17 summarises the relationship between the modelled Moho temperature changes beneath the basin centre to the predicted ΔT_{Moho} (i.e. the 1D-response) as a function of $x_{1/2}$ for the parameter sets in which ΔT_{qc} is positive. Such a parameter set necessarily induces lateral heat flow away from the basin, thereby lowering Moho temperatures beneath the basin centre. For parameter sets in which ΔT_{Moho} is greater than 0 (Fig. 17a), the lateral heat flow is sufficient in about 10% of cases to induce long-term Moho cooling beneath the basin. Provided that $x_{1/2}$ is greater than 100 km most parameter sets show Moho heating exceeds 80% of the predicted ΔT_{Moho} . For parameter sets in which ΔT_{Moho} less than 0, lateral heat flow will augment the Moho cooling beneath the basin, typically by around 10–20%, depending on $x_{1/2}$ (Fig. 17b).

THERMOMECHANICAL SIMULATIONS

In order to assess the way in which the thermal character of the crust and basin-fill may impact on the mechanical response during reactivation we have explored a number of finite element simulations following the approach of Frederiksen & Braun (2001), wherein details of the modelling methodology can be found. Relevant model parameters are listed in Table 2 while results are illustrated in Figs 18 and 19. In each model we have simulated the reactivation of a thermally equilibrated crust incorporating a pre-existing, localised basin with a half-width of 40 km formed as a consequence of stretching by a factor of ~ 1.5 (the thickness of sediment fill in the pre-existing basin is up to 7.7 km, but varies slightly with the imposed thermal parameters). The reactivation following thermal equilibration involves the imposition of a horizontal velocity boundary condition; the modelled lithospheric section has been stretched again at constant velocity of 1 mm yr^{-1} for 25 Ma, followed by thermal relaxation of 50 Ma. The density of the sediment fill is 2350 kg m^{-3} , and

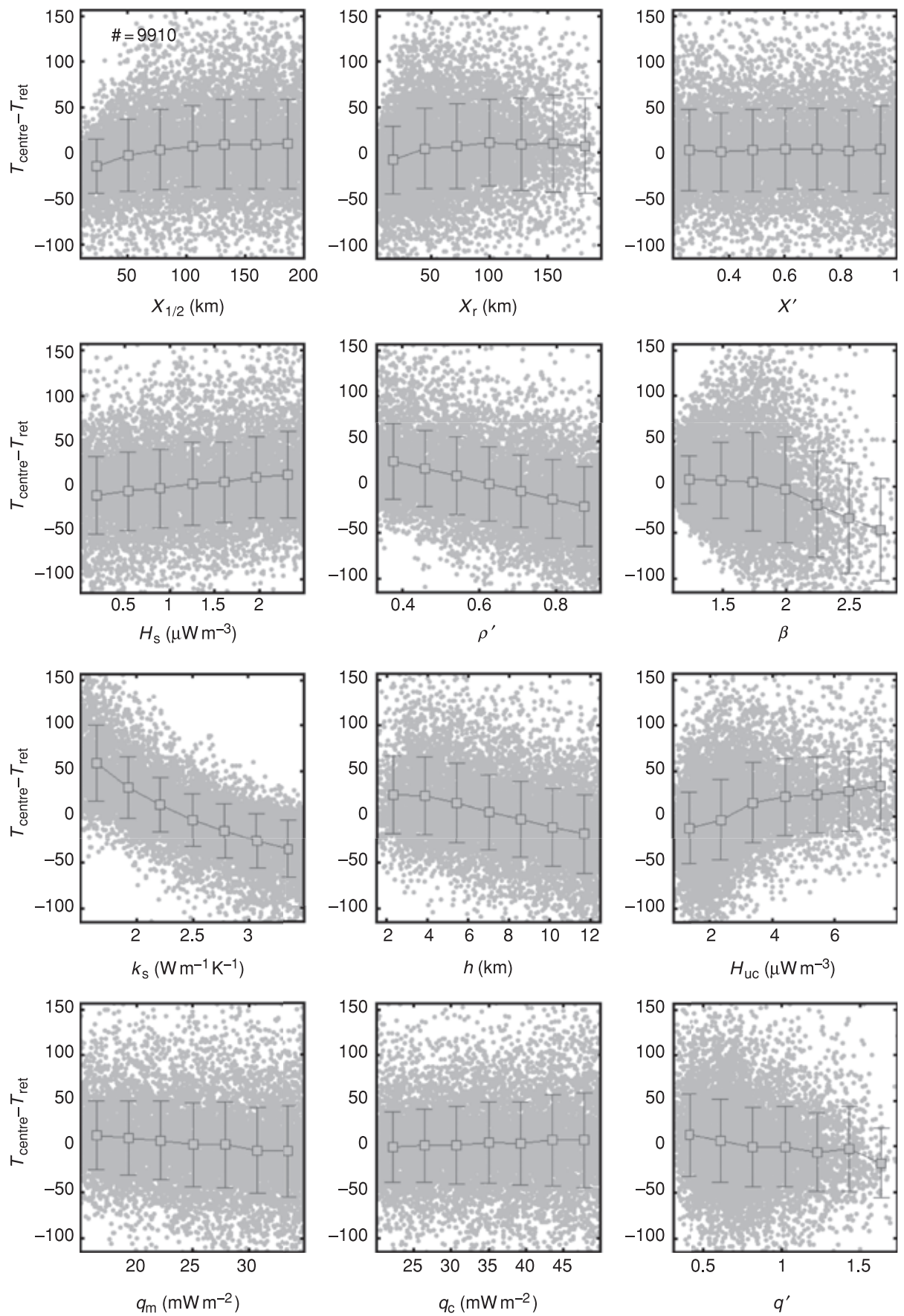


Fig. 13. Results of Monte-Carlo simulation involving $\sim 10\,000$ finite element solutions with variation in basin width and other parameters on the Moho temperature difference between the basin centre and far field.

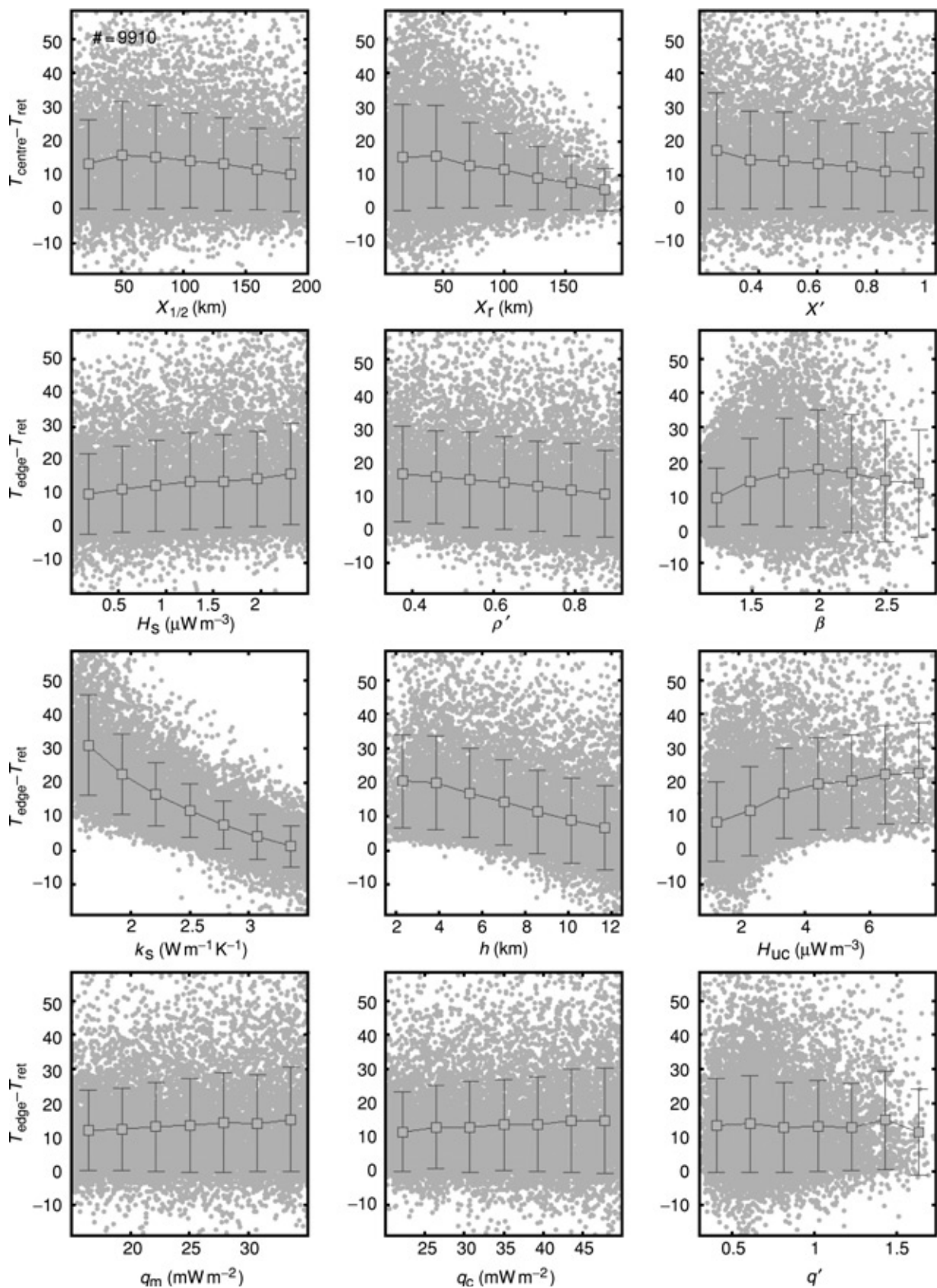


Fig. 14. Results of Monte-Carlo simulation involving $\sim 10\,000$ finite element solutions with variation in basin width and other parameters on the Moho temperature difference between the basin edge and far field.

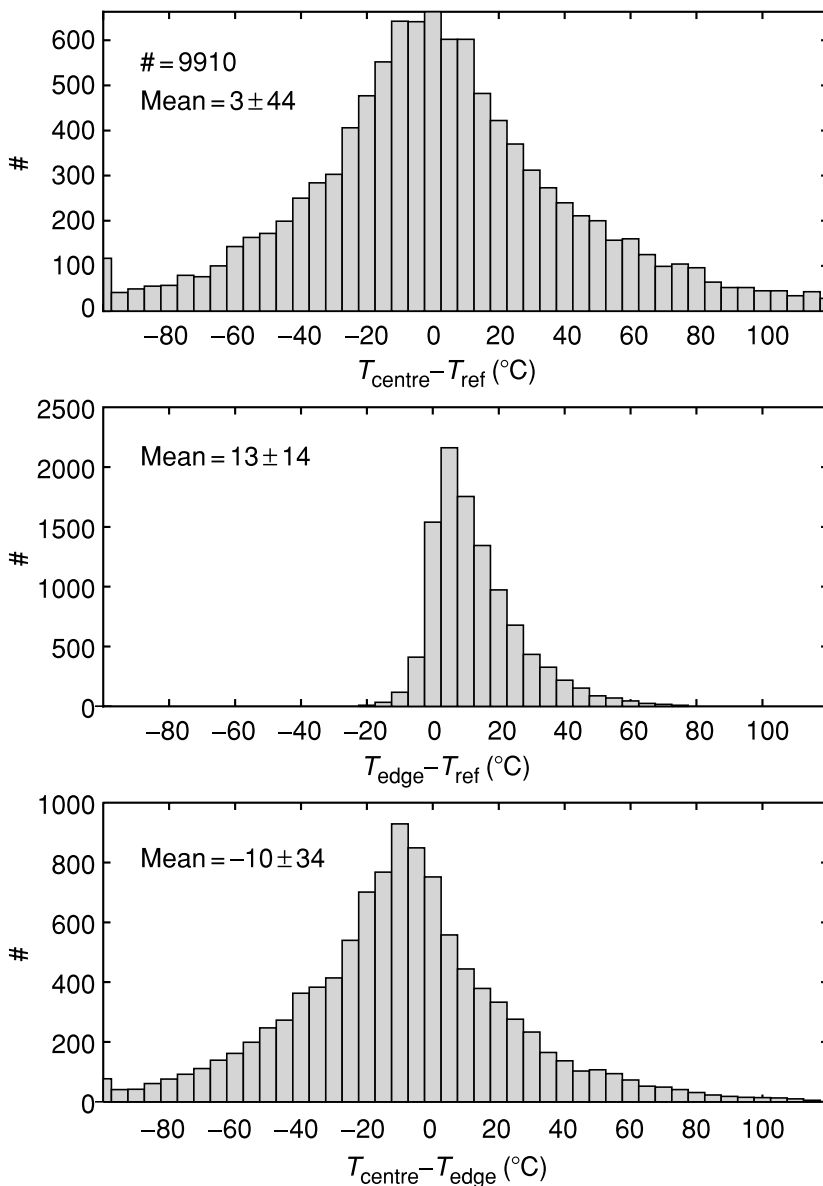


Fig. 15. Histogram summary of Monte-Carlo simulation results.

Table 2. Summary of model parameters used in thermo-mechanical simulations illustrated in Figs 18 and 19.

| Model | Figure | k_s W m ⁻¹ K ⁻¹ | H_c μW m ⁻³ | h km |
|-------|--------|--|-----------------------------|-----------|
| 1 | 18a | 3.0 | 3.0 | 7.5 |
| 2 | 18b | 1.5 | 3.0 | 7.5 |
| 3 | 18c | 3.0 | 1.3 | 17.5 |
| 4 | 18d | 1.5 | 1.3 | 17.5 |

The density of the sediment fill in all models is 2350 kg m⁻³, the sediment heat production is 1.5 μW m⁻³, the mantle heat flow is 25 mW m⁻² and the conductivity of the crust and mantle is 3 W m⁻¹ K⁻¹.

no compaction occurs. The reference crust heat flow contribution, q_c , in all models is 40 mW m⁻³, with the crustal heat production concentrated either in the upper 15 km ($h = 7.5$ km) of the crust, or distributed throughout the crust ($h = 17.5$ km).

For the reference case (Model 1, Fig. 18a), with no conductivity contrast between the basin-fill and the underlying crust, a successor basin is developed above the rift flank of the pre-existing basin, reflecting the localised weakening beneath the rift flank associated with the lateral heat flow from beneath the basin centre. With progressive rifting the locus of deformation migrates toward the hinterland producing an offlap of the successor basin sequences. The fundamental role of the heat production distribution in the pre-existing crust is highlighted by Fig. 18c (Model 3), which differs from Model 1 only in as much as the crustal heat sources are distributed throughout the crust (Table 2). In this instance, initial rift basin formation leads to a reduction in the thermal gradients beneath the basin (Fig. 19a), and therefore to long-term strengthening of the basin and its margins. Consequently, the successor basin avoids the vicinity of the initial basin.

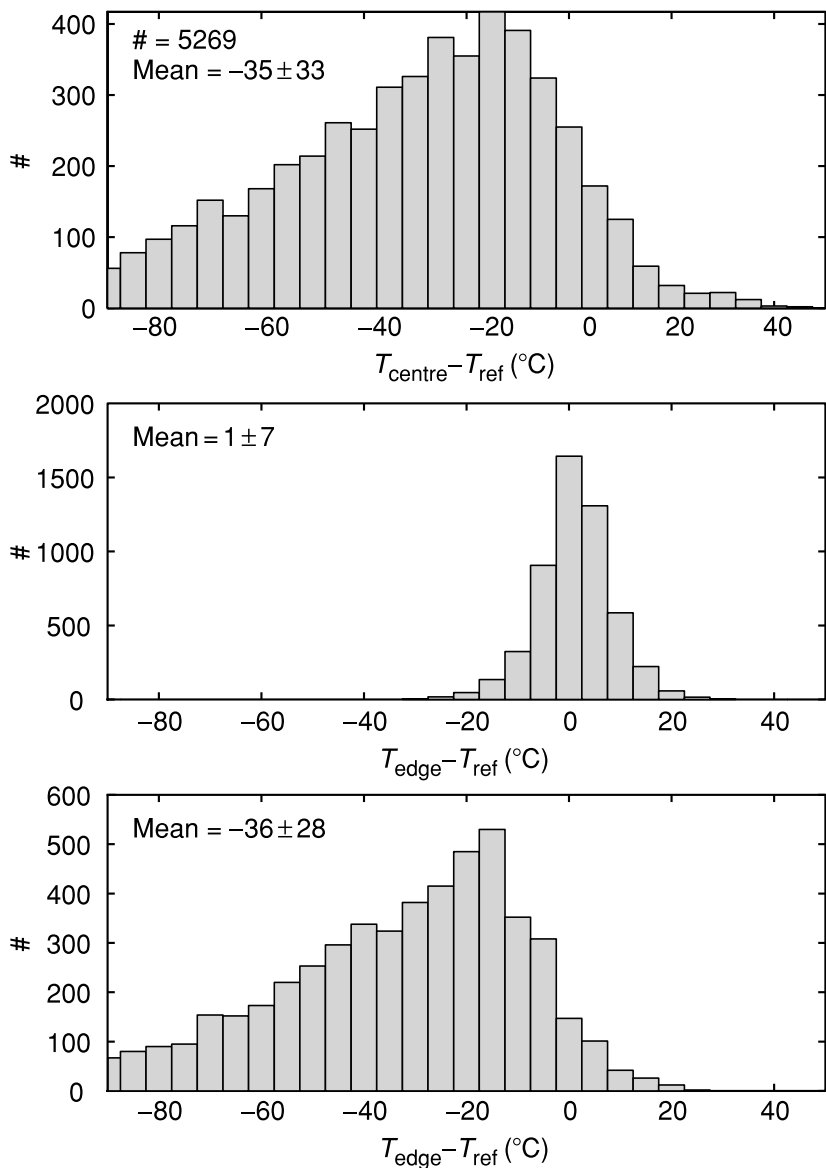


Fig. 16. Histogram representation of the results of a Monte-Carlo simulation involving ~ 5300 solutions with no conductivity contrast between basin-fill and underlying crust.

The overwhelming importance of thermal conductivity of the sediment-fill is indicated by Models 2 and 4, in which the thermal conductivity of the sediment-fill is half that of the underlying crust (otherwise Models 2 and 4 correspond to models 1 and 3, respectively). The steepening of the thermal gradients beneath the basin due to the insulating nature of the fill causes substantial long-term weakening beneath the basin, sufficient to localise successor basin subsidence above the pre-existing basin. Nevertheless, like Models 1 and 3, the successor basin subsidence patterns remain sensitive to the distribution of heat sources in the underlying crust.

DISCUSSION

The calculations summarised in the preceding sections show that there is a potentially large range in the long term thermal response to rift basin formation, reflecting

both the properties and geometry of the basin and its fill as well as thermal property structure of the underlying crust. The long-term thermal response to rifting is particularly sensitive to the distribution of heat sources in the crust, because it is a primary determinant in relative magnitudes of (1) the cooling induced by attenuation of the crustal heat production and (2) the heating induced by the burial of the attenuated crustal heat production beneath the basin-fill. The shallower the distribution of heat sources in the pre-existing crust, the more likely basin formation is to lead to long-term heating, with the consequence that subsequent reactivation will be localised in the vicinity of the existing basin.

For wide basins, with half widths in excess of about 100 km, 1D calculations provide a close approximation to the thermal response of the basin centre. For such wide, sediment-filled basins the most likely long-term thermal response involves (1) cooling of the Moho (by about

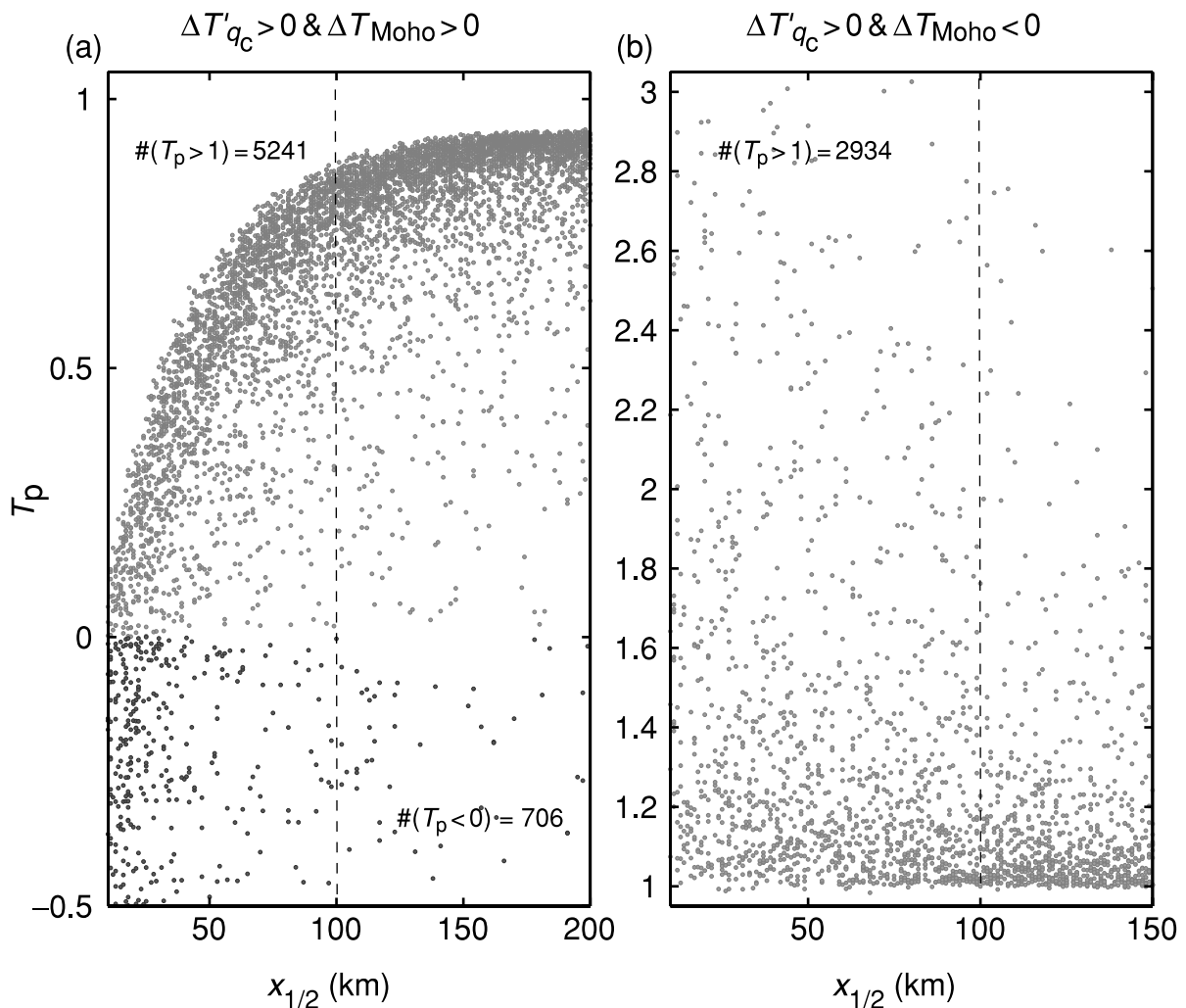


Fig. 17. Illustration of the ratio, T_p , of computed change in Moho temperature beneath a 2D-confined basin centre and the ΔT_{Moho} for the parameter set (i.e. the predicted Moho temperature change in the 1D-limit). Figure 17a shows the parameter sets for which ΔT_{Moho} is greater than 0. Figure 17b shows the parameter set for which the ΔT_{Moho} is less than 0.

20 °C for a β of 1.5) and (2) an increase in the average crustal thermal gradient. In cases where the basin fill is substantially less conductive than the underlying crust, or is relatively dense, basin formation may lead to long-term Moho heating despite the fact that the Moho is shallowed beneath the basin.

Many earlier analyses (e.g. England, 1983; Braun, 1992) overlooked these points because they either ignored crustal heat production or considered that it could be characterised by just one set of $h-q_c$ parameters. The analysis presented herein, extending on the results of Hansen & Nielsen, 2002), and Sandiford (1999), provides a comprehensive analysis of the role of heat production variation on the potential long-term thermal structuring of rift basins. As demonstrated by Hansen & Nielsen (2002), a fundamental consequence of the long-term increase in average crustal thermal gradients following basin formation, is to induce lateral heat flow from beneath the basin

centre towards the basin margin. Such lateral heat flow necessarily reduces the Moho temperatures beneath the basin centre, and heats the Moho in the vicinity of the basin margin, by up to about 30 °C. Our FEM simulations show that such thermal structuring will dictate the distribution of subsequent deformation events, potentially providing an important control on the location of successor basins and, by inference, tectonic inversion. These simulations show that the long-term thermal structuring of the continental lithosphere as a consequence of basin formation may be fundamental to its subsequent mechanical evolution. Consequently, any assessment of the factors responsible for reactivation of basins, during the development of successor basins or during inversion, should consider the long-term thermal consequences of the initial basin forming process. For example, the offset observed in stacked rift basins as shown in Fig. 1, is explicable in terms of a mechanical

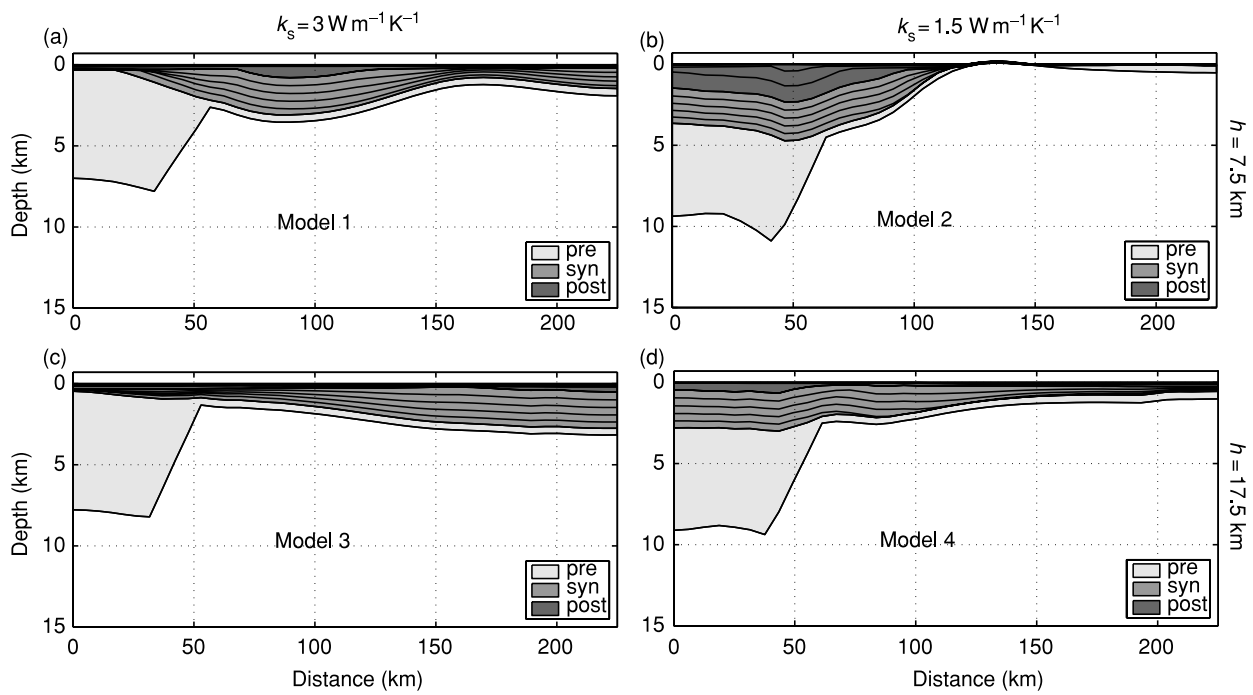


Fig. 18. Illustration of geometries of successor basins, developed by finite element simulation of the stretching of a crust with thermally equilibrated pre-existing basin (see text for discussion). Model parameters are listed in Table 2 ('pre' = pre-existing basin, 'syn' = syn-rift successor basin).

consequences of the thermal structuring of the typical continental crust as illustrated in Fig. 18a, without any appeal to the effects of structural anisotropy or fundamental inherited weakness associated with the initial basin-bounding faults. This is not to say that pre-existing faults are unimportant in reactivation. Rather, it simply highlights the potential ambiguity in the analysis of the factors that control reactivation. This point is worthy of elaboration since much of the literature on basin reactivation has focused on the role of pre-existing structure. In the context of basin reactivation where pre-existing structures in the upper crust are clearly exploited, it is sensible to ask whether such structures are responsible for controlling the localisation of strain at the lithospheric scale, or whether they are exploited when strain is localised by another process such as the thermal and/or compositional structure of the lithosphere. This is related to the question of whether the strength of the lithosphere is dominated by the shallow part of the lithosphere where frictional plastic processes dominate, or in the deeper lithosphere where viscous, temperature dependant creep processes are more likely to dominate. In reality, both processes must contribute, with their relative importance dependant on the thermal compositional and structural character of the lithosphere, and therefore subject to time dependence. One of the main conclusions of our work is that, at least within the context of our present understanding of lithospheric rheology, it is possible to frame many aspects of the lithospheric-scale strain localisation associated with basin reactivation, in terms of

thermal processes. Of course, we would expect that the strain localisation in the shallow, frictional plastic regime will naturally exploit pre-existing structures, and the challenge remains to identify geological observables that will allow us to unambiguously discriminate between the potential factors that contribute to lithospheric strength, and thus localise deformation.

The impact of the length-scale of the HPE distribution on the long-term thermal consequences of rifting raises some important issues concerning the origin of these length-scales. Rifting in response to long-wavelength extensional stress regimes may be expected to exploit weak zones in the lithosphere including those induced by variation in the thermal structure of the lithosphere related to HPE distribution (Sandiford & McLaren, 2002). On the continental scale, we might expect significant regional variations in both h and q_c . All other factors being equal, the hottest Moho temperatures, and potentially weakest crust will correlate with the highest values of h . The localisation of extensional deformation in areas of relatively high- h has the long-term consequence of reducing both h and q_c producing long-term cooling of the Moho. This thermal response will necessarily change the pattern of strength at the continental scale, thereby prejudicing the response during subsequent tectonic episodes. The intriguing possibility raised by this scenario is the suggestion of a profound feedback between continental-scale tectonic activity and the long-term ordering of HPE's in the lithosphere (Sandiford *et al.*, 2001; Sandiford & McLaren, 2002).

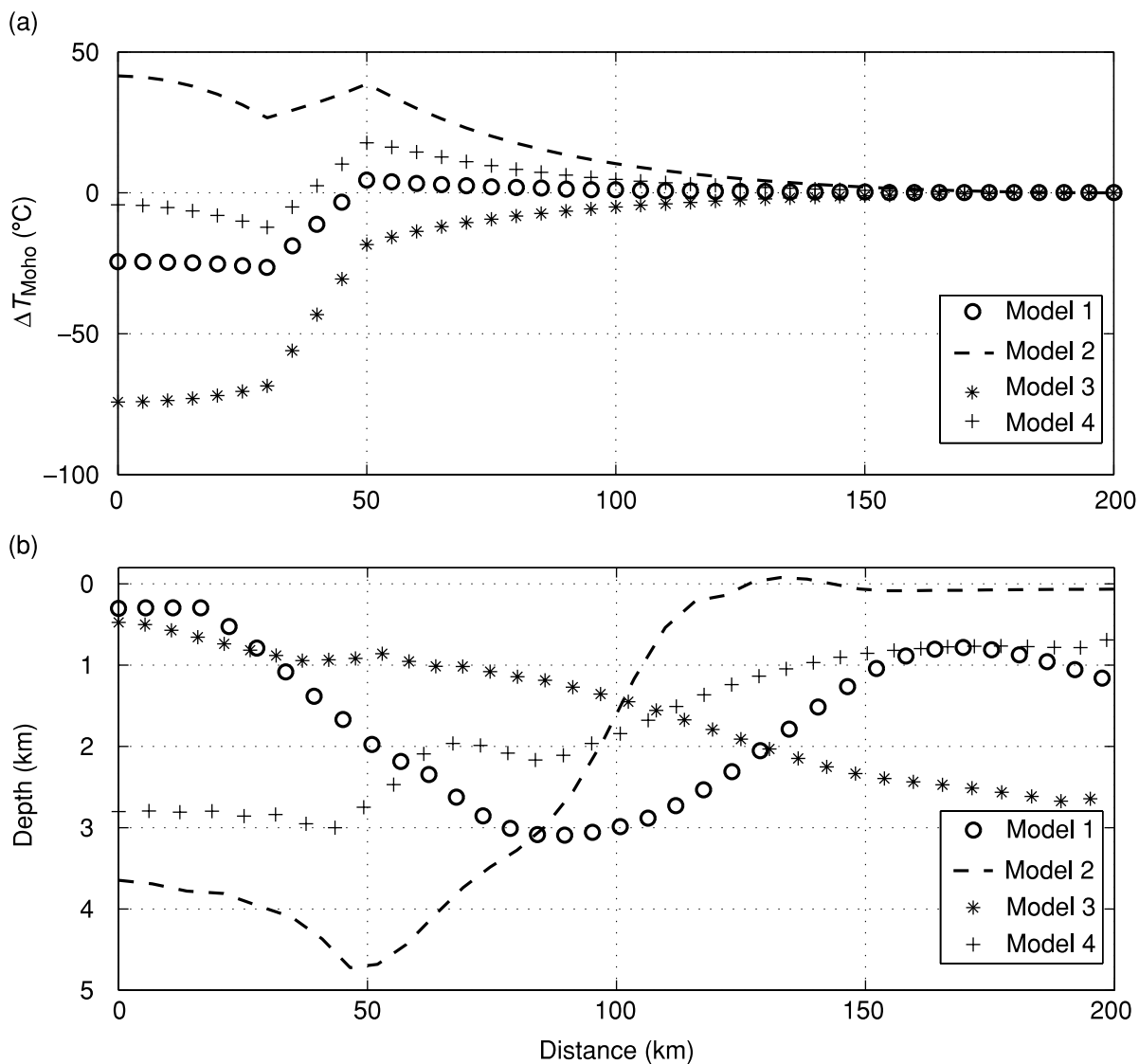


Fig. 19. (a) Moho temperatures along profiles for models shown in Fig. 18. Temperatures have been normalised by subtracting the far-field Moho temperature. (b) Successor basin thickness along profiles for models shown in Fig. 18.

ACKNOWLEDGEMENTS

SF was supported by funds from the Inge Lehman Grant of 1983 and the Danish Natural Science Research Council. P. Burgess, Marlies ter Voorde and an anonymous reviewer are thanked for their reviews.

REFERENCES

- BERTOTTI, G., TER VOORDE, M., CLOETINGH, S. & PICOTTI, V. (1997) Thermomechanical evolution of the South Alpine rifted margin (North Italy): constraints on the strength of passive margins. *Earth Planet. Sci. Lett.*, **146**, 181–193.
- BRACE, W.F. & KOHLSTEDT, D.L. (1980) Limits on lithospheric strength imposed by laboratory experiments. *J. Geophys. Res.*, **85**, 6248–6252.
- BRAUN, J. (1992) Postextensional mantle healing and episodic extension in the Canning basin. *J. Geophys. Res.*, **97**, 8927–8936.
- BUCHANAN, J.G. & BUCHANAN, P.G. (1995) Basin inversion. *Geol. Soc. Spec. Publ.*, **88**, 596.
- COOPER, M.A. & WILLIAMS, G.D. (1989) Inversion tectonics. *Geolo. Soc. Spec. Publ.*, **44**, 375.
- ENGLAND, P.C. (1983) Constraints on extension of continental lithosphere. *J. Geophys. Res.*, **88**, 1145–1152.
- ENGLAND, P.C. (1987) Diffuse continental deformation: length scales, rates and metamorphic evolution. *Philos. Trans. Royal Soc. London*, **A321**, 3–22.
- ENGLAND, P.C., OXBURGH, E.R. & RICHARDSON, S.W. (1980) Heat refraction and heat production in and around granite plutons in northeast England. *Geophys. J. Royal Astronom. Soc.*, **62**, 439–455.
- ERIKSSON, K.A., SIMPSON, E.L. & JACKSON, M.J. (1993) Stratigraphic evolution of a Proterozoic syn-rift to post-rift basin: constraints on the nature of lithospheric extension in the Mount Isa Inlier, Australia. In: *Tectonic Controls and Signatures in Sedimentary Successions* (Ed. by L.E. Frostick & R.J. Steel) *Int. Assoc. Sediment. Spec. Publ.*, **20**, 203–221.
- FREDERIKSEN, S. & BRAUN, J. (2001) Numerical modelling of strain localisation during extension of the continental lithosphere. *Earth Planet. Sci. Lett.*, **188**, 241–251.

- HAENEL, R., RYBACH, L. & STEGENA, L. (1988) Handbook of terrestrial heat-flow density determination. *With Guidelines and Recommendations of the International Heat Flow Commission.* p. 486. Kluwer academic publishers, Dordrecht, Netherlands.
- HANSEN, D. & NIELSEN, S.B. (2002) Does thermal weakening explain basin inversion, stochastic modelling of the thermal structure of sedimentary basins. *Earth Planet. Sci. Lett.*, **198**, 113–127.
- JAUPART, C. (1983) Horizontal heat transfer due to radioactivity contrasts: causes and consequences of the linear heat flow relation. *Geophys. J. Royal Astronom. Soc.*, **75**, 411–435.
- LACHENBRUCH, A.H. (1968) Preliminary geothermal model of the Sierra Nevada. *J. Geophys. Res.*, **73**, 6977–6989.
- LOWELL, J.D. (1995) Mechanics of basin inversion from worldwide examples. *Geol. Soc. Spec. Publ.*, **88**, 39–58.
- MCKENZIE, D.P. (1978) Some remarks on the development of sedimentary basins. *Earth Planet. Sci. Lett.*, **40**, 25–32.
- MCLENNAN, S.M. & TAYLOR, S.R. (1996) Heat flow and the chemical composition of continental crust. *J. Geol.*, **104**, 369–377.
- NIELSEN, S.B. (1987) Steady state heat flow in a random medium and the linear heat flow – heat production relationship. *Geophys. Res. Lett.*, **14**, 318–321.
- O'DEA, M.G., LISTER, G.S., MACCREADY, T., BETTS, P.G., OLIVER, N.H.S., POUND, K.S., HUANG, W. & VALENTE, R.K. (1997) Geodynamic evolution of the Proterozoic Mount Isa terrain. In: *Orogeny Through Time* (Ed. by J.P. Burg & M. Ford) *Geol. Soc. Spec. Publ. London*, **121**, 99–122.
- ORD, A. & HOBBS, B. (1989) The strength of the continental crust. *Tectonophysics*, **158**, 269–289.
- PAUL, E., FLOTTMANN, T. & SANDIFORD, M. (1999) Structural geometry of the northern Flinders Ranges in the Adelaide Fold Belt, South Australia. *Aust. J. Earth Sci.*, **46**, 343–354.
- PEREIRA, E.B., HAMZA, V.M., FURTADO, V. & ADAMSA, J.A.S. (1986) U, Th and K content, heat production and thermal conductivity of Sao Paulo, Brazil, continental shelf sediments, a reconnaissance work. *Chem. Geol.*, **58**, 217–226.
- ROY, R.F., BLACKWELL, D.D. & BIRCH, F. (1968) Heat generation of plutonic rocks and continental heat flow provinces. *Earth Planet. Sci. Lett.*, **5**, 1–12.
- SANDIFORD, M. (1999) Mechanics of basin inversion. *Tectonophysics*, **305**, 109–120.
- SANDIFORD, M., HAND, M. & MCLAREN, S. (2001) Tectonic feedback, intraplate orogeny and the geochemical structure of the crust: a central Australian perspective. In: *'Continental Reactivation and Reworking'* (Ed. by J. Miller, R. Holdsworth, I. Buick & M. Hand). *Geol. Soc. Spec. Publ.*, **184**, 195–218.
- SANDIFORD, M. & MCLAREN, S. (2002.) Tectonic feedback and the ordering of heat producing elements within the continental lithosphere. *Earth Planet. Sci. Lett.*, **204**, 133–150.
- SIBSON, R.H. (1995) Selective fault reactivation during basin inversion: potential for fluid redistribution through fault-valve action. *Geol. Soc. Spec. Publ.*, **88**, 3–20.
- SONDER, L. & ENGLAND, P. (1986) Vertical averages of rheology of the continental lithosphere; relation to thin sheet parameters. *Earth Planet. Sci. Lett.*, **77**, 81–90.
- TER VOORDE, M. & BERTOTTI, G. (1994) Thermal effects of normal faulting during rifted basin formation, 1. A finite difference model. *Tectonophysics*, **240**, 133–144.
- VAN WEES, J.D. & STEPHENSON, R. (1995) Quantitative modelling of basin and rheological evolution of the Iberian Basin (Central Spain): Implications for lithospheric dynamics of intraplate extension and inversion. *Tectonophysics*, **252**, 163–178.
- ZEIGLER, P.A., CLOETINGH, S. & VAN WEES, J.D. (1995) Dynamics of intraplate compressional deformation: the Alpine foreland and other examples. *Tectonophysics*, **252**, 7–59.

APPENDIX

In this appendix we outline the logic that equates the length-scale in Eq. (6), h , to the length-scale for various analytical models for heat production distribution, such as shown in Fig. 2a.

For the case where all crustal heat production is confined to an upper crustal layer of uniform heat production, the temperature field in the layer is given by:

$$T_z = \frac{q_m z}{k} + \frac{H_s z (h_r - z/2)}{k} \quad (\text{A1})$$

where H_s is the characteristic heat production in the heat producing layer, h is the thickness of the heat producing layer, and k is the thermal conductivity. In Eq. (A1) the first term on the right represents the component of the temperature field due to the heat flow from beneath the heat producing parts of the lithosphere (dashed line in Fig. 2b). The second term on the right represents the contribution due to heat sources in the crust and is used to define the quantity, T_{qc} , representing the temperature contribution at any depth due to heat production in the crust. T_{qc} reaches its maximum value (T'_{qc}) at the base of the heat-producing layer. The appropriate expressions for T'_{qc} for this model is therefore:

$$T'_{qc} = \frac{H_s h_r^2}{2k} \quad (\text{A2})$$

Equating Eq. (A2) with Eq. (7), and noting that $q_c = H_s h$, yields $h = h_r/2$.

For a model in which heat production reduces exponentially with depth (i.e. Figure 2a) the appropriate expressions for T'_{qc} is:

$$T'_{qc} = \frac{H_s h_r^2 (1 - \exp(-z_c/h_r))}{k} \quad (\text{A3})$$

where z_c is the depth at which the exponential heat production distribution is terminated, which we approximate as the Moho. Provided that $z_c \gg h$ then Eq. (A3) reduces to:

$$T'_{qc} \approx \frac{H_s h_r^2}{k} \quad (\text{A4})$$

Equating Eq. (A3) with Eq. (7) yields $h = h(1 - \exp(-z_c/h))$ which reduces to $h = h$ for $z_c \gg h$.

Manuscript received 10 January 2002; Manuscript revised 26 October 2002; Manuscript accepted 26 November 2002.